MTL TR 92-55

AN INTRODUCTION TO MOIRE METHODS WITH APPLICATIONS IN COMPOSITE MATERIALS

ROBERT F. ANASTASI
MATERIALS TESTING AND EVALUATION BRANCH

August 1992

US ARMY
LABORATORY COMMAND
MATERIALS TECHNOLOGY LABORATORY

U.S. ARMY MATERIALS TECHNOLOGY LABORATORY
Watertown, Massachusetts 02172-0001

The findings in this report are not to be construed as an official Department of the Army position, unless so designated by other authorized documents.

Mention of any trade names or manufacturers in this report shall not be construed as advertising nor as an official indorsement or approval of such products or companies by the United States Government.

DISPOSITION INSTRUCTIONS

Destroy this report when it is no longer needed.
Do not return it to the originator

UNCLASSIFIED

SECURITY CLASSIFICATION OF THIS PAGE *(When Data Entered)*

REPORT DOCUMENTATION PAGE		READ INSTRUCTIONS BEFORE COMPLETING FORM
1. REPORT NUMBER MTL TR 92-55	2. GOVT ACCESSION NO.	3. RECIPIENT'S CATALOG NUMBER
4. TITLE *(and Subtitle)* AN INTRODUCTION TO MOIRE METHODS WITH APPLICATIONS IN COMPOSITE MATERIALS		5. TYPE OF REPORT & PERIOD COVERED Final Report 6. PERFORMING ORG. REPORT NUMBER
7. AUTHOR*(s)* Robert F. Anastasi		8. CONTRACT OR GRANT NUMBER*(s)*
9. PERFORMING ORGANIZATION NAME AND ADDRESS U.S. Army Materials Technology Laboratory Watertown, Massachusetts 02172-0001 SLCMT-MRM		10. PROGRAM ELEMENT, PROJECT, TASK AREA & WORK UNIT NUMBERS
11. CONTROLLING OFFICE NAME AND ADDRESS U.S. Army Laboratory Command 2800 Powder Mill Road Adelphi, Maryland 20783-1145		12. REPORT DATE August 1992 13. NUMBER OF PAGES 55
14. MONITORING AGENCY NAME & ADDRESS *(if different from Controlling Office)*		15. SECURITY CLASS. *(of this report)* Unclassified 15a. DECLASSIFICATION/DOWNGRADING SCHEDULE

16. DISTRIBUTION STATEMENT *(of this Report)*

Approved for public release; distribution unlimited.

17. DISTRIBUTION STATEMENT *(of the abstract entered in Block 20, if different from Report)*

18. SUPPLEMENTARY NOTES

19. KEY WORDS *(Continue on reverse side if necessary and identify by block number)*

Moire analysis
Composite materials
Optical methods
Laminates

20. ABSTRACT *(Continue on reverse side if necessary and identify by block number)*

(SEE REVERSE SIDE)

DD FORM 1 JAN 73 1473 EDITION OF 1 NOV 65 IS OBSOLETE

UNCLASSIFIED

SECURITY CLASSIFICATION OF THIS PAGE *(When Data Entered)*

Block No. 20

ABSTRACT

The moire effect or the fringe pattern formed by superimposing two arrays of dark and light line patterns is utilized in experimental mechanics to measure deformations of bodies subjected to external loads. Although mainly a laboratory tool the techniques have been applied to problems in the mechanics of composite materials to map strain concentrations around holes, cracks, and delamination, as well as examining edge effects, shearing deformation, and mechanically fastened composite material.

CONTENTS

INTRODUCTION

The moire effect is utilized in experimental mechanics to measure the deformation of bodies subjected to external loads. Deformations are viewed as contour maps of displacement and are referred to as fringe patterns. In-plane and out-of-plane displacement fringe patterns can be generated using techniques of geometric moire, shadow moire, and interferometric moire. This paper describes these methods and surveys their application to composite material.

Geometric Moire

A moire fringe pattern is formed by superimposing two gratings: one undistorted, and one distorted due to specimen deformation; detailed references are given by Theocaris, Durelli, Chiang, and Parks.[1-4] Gratings are arrays of dark and light lines usually straight, parallel, and equally spaced; examples are shown in Figure 1. When two line gratings of different pitch (line spacing) are superimposed without rotation, then moire fringes will be formed that represent the different pitch, as shown in Figure 2. When two gratings of equal pitch with a rotation between are superimposed, the moire fringe pattern shown in Figure 3 is obtained. Generally, a deformed grating is a combination of elongation and rotation resulting in moire fringes that represent lines of equal displacement, as shown in Figure 4.

One grating attached to a specimen surface is referred to as the specimen grating and is normally applied with grating lines parallel or normal to specimen axes. The resulting fringe patterns are governed by the equation:

$$U = \frac{N}{f} \tag{1}$$

where U is the displacement component in the direction perpendicular to the lines of the reference grating, N is the fringe order number, and f is the frequency of the reference grating (inverse of the pitch).

In practice, a cross grating is used as the specimen grating and allows two perpendicular displacement fields to be obtained. Typically, the cross grating is oriented along the principal x and y axes to obtained U and V displacement fields. A line grating reference may be used to seperate U and V displacement patterns by positioning it over the specimen grating first in the x direction then rotating it 90^{o} to obtain the y direction pattern. A cross grating reference may also be used to obtain both U and V patterns simultaneously, then techniques of optical spatial filtering are used to separate the family of fringes (see Chiang[5]).

From the U and V displacement fields, strain at any point on the specimen surface can be determined. Using small displacement assumptions; i.e., neglecting higher order derivatives, the strain displacement relationships are:

$$\varepsilon_x = \frac{\partial U}{\partial x}$$

$$\varepsilon_y = \frac{\partial V}{\partial y} \tag{2}$$

$$\varepsilon_{xy} = \frac{\partial U}{\partial y} + \frac{\partial V}{\partial x}$$

where ε_x and ε_y are normal strains in the x and y directions, respectively, and ε_{xy} is the shear strain in the xy plane. Using the governing equation of moire, Equation 1, and the strain displacement, Equation 2, displacements in the x and y directions can be found as:

$$U = \frac{N_x}{f}$$

$$V = \frac{N_y}{f} \tag{3}$$

where N_x and N_y are fringe orders in the x direction and y direction, respectively, then strains can be found using the following displacement derivatives:

$$\frac{\partial U}{\partial x} = \frac{1}{f}\frac{\partial N_x}{\partial x}$$

$$\frac{\partial U}{\partial y} = \frac{1}{f}\frac{\partial N_x}{\partial y}$$

$$\frac{\partial V}{\partial x} = \frac{1}{f}\frac{\partial N_y}{\partial x} \tag{4}$$

$$\frac{\partial V}{\partial y} = \frac{1}{f}\frac{\partial N_y}{\partial y}$$

The displacement derivatives above are found by ordering the fringes, plotting fringe order versus position, and then taking the slope of the plot at each point where the strain is required. This procedure is illustrated in Figure 5. To increase accuracy, half or fractional fringe orders can be used, as mentioned in Reference 1, where a microdensitometer was used to locate the fractional fringe orders. Today, optical-electronic systems are used and video images are digitized and processed by host computer, as noted by Voloshin.[6]

Shadow Moire

Shadow moire is a method used to map out-of-plane contours of a surface (see Parks[4] and Chiang[7]). This method involves placing a grating of pitch P in front of the surface to be contoured and then illuminating it with collimated light. When this grating and the shadow of this grating are viewed together, an interference pattern is produced that is the out-of-plane contour map of the surface. Contour intervals of the out-of-plane displacements can be obtained by analysis of the moire system, as shown in Figure 6.

The out-of-plane deflection W at a general point A is:

$$W = \frac{NP}{\mathrm{Tan}(\alpha) + \mathrm{Tan}(\beta)} \tag{5}$$

where N is the fringe order and α and β are angles of illumination and viewing, respectively.

Interferometric Moire

Moire interferometry is a highly sensitive full field optical method used to measure in-plane displacements. A high frequency diffraction grating is replicated on the specimen surface and interferes with a reference grating produced by the interference of two collimated beams of laser light. The interference pattern is a moire fringe pattern governed by Equation 1. Details of this moire method can be found in papers by Post[8-12] and Basehore.[13]

The basic difference between geometric and interferometric moire is the frequency of the gratings used. Typical gratings for geometric moire are 1000 lines per inch (lpi) while those of interferometric moire are 30,480 lpi and 60,960 lpi and where high frequency grating of 101,600 lpi have been utilized by Weissman and Post[14] and an ultra-high frequency method has been described by Han and Post[15] with possible extensions to 500,000 lpi or more.

The basic setup of moire interferometry is illustrated in Figure 7 where warped wave fronts A" and B" interfere to form a moire pattern depicted in Figure 8.

Diffraction gratings can be either line gratings or cross gratings, just as in geometric moire, and can be either an amplitude or phase type as illustrated in Figure 9. The amplitude gratings have opaque bars and transparent spaces or vise versa and phase gratings have furrowed surfaces and can be transmissive or reflective.

The replication of high-frequency, highly-reflective diffraction gratings onto a specimen surface has been the technological key in making moire interferometry a valuable measurement tool. The replication process described by Basehore[16] is shown schematically in Figure 10. The replication process starts by exposing a holographic glass plate film to two intersecting beams of coherent illumination; see Figure 11 where the angle of intersection defines the frequency of the interference pattern as:

$$f = \frac{2\,\mathrm{Sin}\,(a)}{\lambda} \qquad (6)$$

where f is the frequency of the interference pattern, λ is the wavelength of light employed, and "a" is half the angle of intersection. When the glass plate film is developed, silver grains remain in the exposed zones while silver is bleached out elsewhere. Upon drying, shrinkage is retrained locally by the silver rich zones resulting in a regular corrugated surface. The film is then dipped in a photo flow solution which leaves a thin layer of contamination on the film surface over which a thin layer of aluminum is deposited. Next, puddle of adhesive is placed on the specimen and the aluminum-coated film is pressed into the adhesive and allowed to cure. Upon curing, the glass film is pried off leaving behind an aluminum layer of corrugated shape, the specimen diffraction grating. The contaminated layer acts as a mold release between the emulsion on the glass plate and the aluminum. Cross-line diffraction gratings are made in a similar manner with an added 90^{0} rotation of the photographic plate and second exposure to the virtual grating.

Another method proposed and demonstrated by Anastasi, et al.[17] involves coating the specimen surface with photo resist, exposing it to a virtual grating of the desired frequency, developing the photo resist, and then overcoating it with a thin layer of aluminum. This procedure eliminates the need for creating the high frequency mold on a photographic glass plate film and the transfer process.

The most commonly used optical arrangement for creating a virtual reference grating is schematically shown in Figure 12 where a lens is shown as a means of collimating the laser beam; however, a parabolic mirror may also be used. Half the collimated beam impinges directly on the specimen surface while the other half is reflected off the mirror. The camera is normal to the specimen surface and records the moire images. A multiple beam arrangement is shown in Figure 13 where a cross-line specimen grating is used and horizontal or vertical reference gratings are produced by choosing pairs of collimated beams to interfere. This arrangement makes possible the recording of U and V fringe patterns without rotation of the specimen. Two additional optical arrangements are shown in Figures 14 and 15 and a proposed optical arrangement for ultra-high frequency moire is shown in Figure 16.

The use of carrier patterns is analogous to mismatch methods in geometric moire Chiang[3] and Parks[4] used primarily to increase the accuracy of extracted data from fringe patterns. Other uses include resolving displacement sign, determination of fringe gradients, and canceling initial no-load fringe patterns. Examples of carrier pattern usage in moire interferometry are demonstrated by Guo.[18]

Fringe Analysis

Absolute fringe orders in strain analysis are not important. As illustrated in Equation 4, the difference in fringe orders are used, not the absolute value. Although if displacements are known from experimental conditions, then fringe orders may be relatively numbered. Fringes are assigned consecutively increasing orders for positive displacements and decreasing if negative. Two neighboring fringes can be of the same order if they are on opposite sides of a hill or valley and fringes of the same order may branch but never intersect or cross. These fringe ordering rules and analysis can be preformed by hand but is a tedious and time consuming task. Computer fringe analysis including hardware and software requirements are discussed by Ranson,[19] Sciammarella,[20] Chanudry,[21] Ning,[22] and Lee.[23] Other computation techniques address noise reduction by digital filtering and least square splines to increasing accuracy of locating fringe centers as noted by Oplinger.[24] New advanced methods employ finite element methods for two-dimensional smoothing and generation of displacement and strain fields as discussed by Segalman[25] and Tessler, et al.[26] A hybrid approach by Gilbert[27] uses the experimental fringe displacements as boundary conditions in a finite element analysis. The approach is said to reduce computational requirements.

MOIRE METHODS APPLIED TO COMPOSITES

Moire methods have been used as a measurement tool for more than 30 years on materials such as paperboard, plastic, rubber, metal, and composites and have been able to provide *whole-field* information as opposed to the information provided by a strain gauge at a single point that may miss localized damage or strain concentrations occurring in unsuspected locations. Basic mechanics concepts governing the behavior of composite materials can be found in the following references: Grimes and Griemann,[28] Halpin,[29] Jones,[30] and Tsai.[31,32]

Presently, moire interferometry is the dominate *whole-field* technique being used in experimental mechanics today. This is due to its high sensitivity that yields numerous fringes for relatively low strain levels; however, geometric and shadow moire still have their place as measurement tools. A survey of how these methods have been applied to composite materials is divided into the following areas: edge effects, damage, holes, shear, and mechanical fastening.

An additional *other* category includes residual strain, nonuniformities, and dynamic measurement applications.

Edge Effects

Edge effects in composites are associated with shear transfer between layers. Severe edge effects cause premature failure or delamination, particularly under fatigue loading. Moire methods, both geometric and interferometric, have been used to obtain face and edge displacements fields in symmetric angle-ply laminates under extensional loading described by Pipes and Daniel,[33] Oplinger, et al.,[34,35] Czarnek, et al.,[36] and Herakovish and Post.[37] The early experimental work was aimed at verifying the work of Pipes and Pagano[38] who developed an elasticity solution to this problem. Later work compared experimental to finite element analysis.

Faces and edges of 8 ply and 16 ply graphite epoxy and boron epoxy composite coupons in tension were examined at angle layups of 10^{o}, 20^{o}, 30^{o}, and 45^{o}. Typical face and edge fringe patterns are shown in Figure 17 where specimen dimensions are 6.0" x 0.4" x 0.04". The experimental moire results plotted along with the theoretical and numerical results in Figure 18 validate the elastic solution of Pipes and Pagano.[38]

Other examples of edge effects can be seen in a thermal strain analysis by Ifju and Post[39] and in a compression test of a thick composite by Wang, Dai, and Post.[40] In both studies the specimen was cut from a thick walled pressure vessel of graphite epoxy $[90_2/0]_{27}$, where 0^{o} fibers were parallel to the axes of the cylinder and the 90^{o} fibers were parallel to the hoop direction. In the thermal study, a specimen grating was replicated on the composite specimen at its stress-free cure temperature of about 250^{o}F then, after cooling deformations were obtained, at room temperature, as shown in Figure 19. Here, the strain is shown to be essentially constant through the central region while edge effect zones can be seen along the vertical boundaries. The authors stated the zone width is equal to two to four ply thicknesses. In the compression study similar displacements were obtained showing shear displacements along vertical boundaries and out-of-plane displacements were obtained using Twyman-Green interferometer. Interlamina properties, modulus of elasticity, and Poisson's ratio were obtained from U, V, and W fringe patterns.

An internal free edge, a hole, in a composite laminate was examined by Borman, Czarnek, and Post.[41] This was an experimental demonstration showing the capability of moire interferometry to record the deformations on the hole surface. The authors stated the most difficult challenge was to replicate the grating inside the 1" diameter hole. A fringe pattern in Figure 20 shows the effect of some local strain concentrations that may be caused by the ply-to-ply response, edge effects, a nonuniform grating on the curved surface, or fiber breakage damage due to drilling.

Damage

Damage such as fiber breakage or delamination in composite may arise from impact or manufacturing defects and can reduce the load carrying capability of structural components. Moire methods are used here in detecting the effect of such damage in tensile and compressive loaded coupons. Damage is detected in tensile loaded coupons by observing fringe concentrations in U and/or V replacement fields. For compression loaded coupons, shadow moire has been used to measure the extent of damage and buckling deformation.

McDonach, et al.[42] demonstrated the use of moire interferometry on detecting the effect of a local impact in a carbon fiber composite material. In this application the carbon composite specimen was then cycled under tensile load. A specimen grating was then applied and fringe patterns were obtained showing strain concentrations and associated damage (see Figure 21a).

The onset of damage was detected by Wood[43] using moire interferometry. A damage load was found for a tensile loaded graphite specimen, $[(\pm 30)_2/(90)]_s$. Subsequent specimens were loaded near this critical load, then U and V displacement fields were obtained. An example is shown in Figure 21b where V displacement fields are shown before and after damage; this is evident in the high concentration of fringes near the edge of the laminate.

The effects of delamination in carbon fiber epoxy and graphite specimens were examined by Mousley[44] and Jones, et al.,[45] respectively. In both studies delaminations were manufactured into specimens by inserting a teflon disk between two plies in the layup process. The specimens were loaded in compression while buckling deformations were recorded by shadow moire. An example is shown in Figure 22 where buckling at two load levels is shown. The high load level shows increased fringe density (increased out-of-plane deflection) and delamination growth (increased area).

Buckling of composite structures was examined by Schwarz[46] where the objective was to determine the onset of buckling in composite panels, stiffened by hat sections and loaded in shear, stiffened by hat sections and loaded in axial compression, and stiffened by semi-sine wave webs loaded in axial compression. Buckling onset was defined as the load at which a wave fringe pattern was observed to have formed across the full width or depth of the structural component.

Holes

Mechanically cut holes are needed in structural materials for bolting or gaining access to the other side of the material. In both cases high stress/strain concentrations exist in the vicinity of the hole for loaded structures. Strain distributions around holes can be found if stress/strain relations are known.

Daniel and Rowlands[47] obtained strain concentrations for 0.50", 0.75", and 1.00" diameter holes in glass epoxy laminates of $[90/0/90/0]_s$ layup. Moire patterns for increasing load levels were obtained and analyzed for far field and maximum strains around the hole. Experimental stress concentration factors were found and compared to theoretical calculations. Results are shown in Figure 23 where the experimental curve tends to have the same shape as the theoretical one for the isotropic case. In another study by Daniel, Rowlands, and Post,[48] strain distributions around a hole were found using fringe multiplication to increase sensitivity and compared to theory; results are shown in Figure 24.

Moire interferometry was demonstrated by Post[49] and Asundi and Cheung[50] to be capable of recording U, V, and W displacement fields around fatigued coupons with central holes. Results show the effect of the outer ply orientation and direction of crack propagation in Figure 25 and residual in-plane and out-of-plane displacements in Figure 26. No quantitative conclusions were made in either of these demonstrations; however, these studies showed a serious degradation of fatigue strength for composite coupons with central holes.

A metal matrix specimen of boron/aluminum $[0/\pm45]_s$ with a central slot was investigated by Post, Czarnek, Jon, and Guo.[51] Moire fringe patterns were obtained for increasing load steps. Fringes of U and V displacement and a plot of strains along the y-axis tangent to the end of the slot are shown in Figure 27. The authors stated that peak shear strain was near 8% for the 80% load level, far into the plastic range of the matrix material.

Shear

Determination of shear modulus and shear strength can be divided into three types:

- In-plane shear in which shear deformation that takes place entirely in the plane of the composite material.
- Twisting shear in which the cross section of the composite undergoes a twisting type deformation.
- Thickness shear (transverse or interlamina shear) in which the composite material sheet undergoes shearing deformation in a plane normal to the plane of the sheet.

Some specimen geometries for the three types of shearing are bending specimens (sheet or beam), torsion tubes, rail shear, Iosipescu, and $\pm$ 45^{o} laminates. From these various geometries moire interferometry has been used with bending, rail shear type loading, and Iosipescu shear tests.

In the bending tests, Post, et al.[52-54] used graphite epoxy beams of $[0]_{48}$ and quasi-isotropic $[45/0/-45/90]_{6s}$ layups under three and five point loading. The horizontal distance between loading points was about twice the specimen thickness. The resulting fringes in Figure 28 show a zigzag or cyclic pattern. The authors state this is due to the existence of thin resin-rich layers that have much less shear stiffness than the fiber material.

A rail shear type of loading was performed by Post, et al.[55] on graphite/epoxy specimens cut from a thick-walled cylinder and cemented to steel rails for shear loading. The specimen configuration U and V displacement fields and shear strain information along typical 0^{o} and 90^{o} plies are shown in Figure 29. Carrier fringes were used to extract the shear strain information. Two specimen configurations were examined; one with a restricting end condition, and the other with a tapered end condition to alleviate abrupt load transfer and stress concentrations. The shear strains were more nearly constant for the tapered end condition but were more concentrated in the central area. Thus, the specimens with restricting end conditions had a nearly constant shear strain along its full length and is, therefore, a superior specimen design.

Moire studies using Iosipescu shear specimens have been performed to evaluate the test method, compare Iosipescu specimens to double notched specimens, and combined experimental/analytical studies.

The test method evaluation by Abdallah, et al.[56] was done on 0.24" thick 0^{o} and 0/90^{o} graphite/epoxy specimens. Moire results in Figure 30 show symmetry of the fringes and areas of constant fringe spacing except the 0^{o} U displacement field that shows an intersection between fiber and matrix. The area of constant shear strain is quite small and the authors state care should be taken in positioning and selecting sizes of strain gage rosettes.

The comparison study by Ifju and Post[57] was done on a thick-walled cylinder specimen of graphite/epoxy $[90_2/0]_9$. Two specimen geometries were cut and tested; an Iosipescu geometry and a double notch geometry. Resulting fringe patterns are shown in Figure 31. In the central test area fringes are closely spaced and vertical in direction. A shear strain distribution was extracted along a line connecting the notch tips. The resulting plot in Figure 32 shows a more uniform shear distribution for the compact double-notched specimen than the Iosipescu specimen, thus, the double-notch specimen is better suited for shear testing.

The combined experimental/analytical investigation by Pindera, Ifju, and Post[58] examined deformation and stress fields in graphite/epoxy and boron/aluminum Iosipescu specimens. The specimens were unidirectional 0^o and 90^o and the boron/aluminum was both annealed and nonannealed. Shear strains in the specimen test sections were calculated from moire patterns and graphed along with finite element analysis results; these are shown in Figure 33. There was a very good correlation between the 0^o and 90^o graphite/epoxy specimens while the boron/alumina showed a poor correlation. The authors suggested a nonlinear finite analysis would improve this correlation. At high load levels the boron/aluminum U-field displacement pattern exhibited a zigzag feature, as shown in Figure 34. This feature was on the order of the boron fiber diameter and was more pronounced in the annealed specimen than in the nonannealed specimen.

Mechanically Fastened

Fasteners such as rivets, bolts, and pins are used to attach composites to composites or composites to metals. Factors that influenced the design of these joints (from the composite point of view) are anisotropic stiffness, interlamina shear, and fiber type and form such as random, woven, and unidirectional. Other influencing factors are geometry (width, end distance, laminate thickness, and bolt diameter), bolt fit or tolerance, washer size, clamping force, and type of load that is static, dynamic, or cyclic. These factors are commonly examined experimentally on single bolt specimens loaded in double shear and tested to failure. Modes of failure consist of bolt bending, bolt shear, tension, shear-out, bearing, and cleavage-tension. The last four of these are shown schematically in Figure 35.

Moire has primarily been used to examine the strain distribution around single pin loaded joints for various fiber orientations. Other uses have been to examine contact stresses between pin and composite, multiple pin loading, stress concentration relief, and effects due to load spreading washers.

Oplinger,[59] Koshide,[60] and Serabian and Oplinger[61] used geometric moire to examine the strain distribution around single pin loaded joints. Oplinger's investigation included an analytical two-dimensional linear elastic boundary collocation scheme. Comparison of this analytical scheme to moire showed that a $0/90^o$ glass epoxy laminate was nonlinear in shear along a prescribed locus of maximum shear strains (see Figure 36). Results also showed failures may occur along lines having the same shape of the locus of maximum shear strain. Koshide investigated the correlation between strain distribution and fiber orientation. Specimens were graphite/epoxy cross-plied and woven-fabric. The fringe patterns for two load levels are shown in Figure 37 along with the specimen and loading configurations. Bearing and net section longitudinal strains were obtained for two load levels; results are shown in Figure 38. The authors stated that strain distributions were shown by moire to be influenced by orientation of fiber to load direction and shearing deformation arose in the $0/90^o$ specimens but not the $\pm 45^o$ specimens. Serabian and Oplinger[61] examined the response of S-glass/epoxy

specimens $[0/90)_{3},0]_s$ and confirmed earlier work that nonlinear response must be taken into account in stress analysis. A finite element analysis using nonlinear material properties with a two-dimensional version of Hoffman's failure criterion highlighted the nonlinear effects of material softening (see Figure 39).

Contact stresses in pin-loaded plates were investigated by Tsai, et al.[62] Moire interferometry was used to obtain deformation fields very close to the pin-plate contact area allowing the frictional nature of the contact to be examined. The specimen was graphite/epoxy $[0_2/60_2-60_2]_s$ with the 0^o fibers parallel to the loading direction. The hole was cut with a diamond core drill for pin clearance fit of 0.001". Resulting U- and V-field fringe patterns and contact stress distributions are shown in Figure 40. An aluminum specimen was also tested and showed similar stress distributions.

Cloud, et al.[63-66] used moire interferometry to investigate, stress concentration relief, two fasteners in parallel and perpendicular to load direction, and effects due to load spreading washers. The stress concentration relief study compared the effects of inserting thin bands of plastic and aluminum in the hole of the pin loaded coupon. This showed it is possible to reduce by approximately 90% the stress and strain concentration factors by inclusion of a thin band of material having properties stiffer than the laminate. In the two fastener studies, results showed reduction of stress concentration compared to a single fastener with the parallel arrangement outperforming the perpendicular one. The load spreading study evaluated the possibility of obtaining significant strain relief through the use of flat or conical load spreading washers in combination with high and low torque. The high torque case performed better than the low torque case and conical washers concave side up offered the best degree of strain relief.

Other

Some applications of moire that did not fall into any of the categories mentioned above examine residual strain, nonuniformities, and dynamic measurements.

The residual strain investigation was done by Lee, Czarnek, and Guo[67] and Morton and Post.[68] They used moire interferometry for in-plane measurements and a Twyman-Green interferometer for out-of-plane measurements. The specimen was a thick graphite/epoxy ring cut from a cylinder with a $0/90^o$ layup of sequence $[90_2/0)_{29}/90_2]$. Moire fringes were obtained while the specimen was sliced and undercut to relieve stresses (see Figure 41). The magnitude of the residual strain was found to be on the order of 25% of the ultimate strain of the material.

Nonuniformities in a composite panel was examined by Czarnek, Post, and Guo.[69] They loaded a panel in tension then adjusted a mirror in the optical arrangement to cancel the uniform part of the fringe pattern. The remaining pattern showed irregularities across the panel, as shown in Figure 42. While most of the uniformities were randomly scattered across the panel, there was a band showing some imperfection along a lamina orientation that could have been caused by manufacturing defects, such as variations in fiber distributions or fiber matrix volume. This method could be used for quality control inspection or a way to examine variations in material fabrication processes.

Dynamic applications of moire were done by Armenakas and Sciammarella,[70] Epstein, Deason, and Abdallah,[71,72] as well as Hsu, Liu, Chiang, and Anastasi.[73] Armenakas and Sciammarella examined the response of glass/epoxy specimens to high strain rates of tensile load up to 30,000 in./in./min. The results showed a linear response of the modulus when plotted against strain rate on a logarithmic scale. Epstein used moire interferometry to study the transient wave propagation on the free surface of a 48-ply graphite/epoxy $[0/90]_s$ specimen impact geometry, and resulting fringe patterns are shown in Figure 43. A shear effect seen in the fringe patterns results from modulus and wave speed differences in the 0^o and 90^o layers. Hsu used geometric moire coupled with a high speed digital camera and pulsed copper vapor laser to examine the fracture toughness of a glass/epoxy compact tension specimen. This study demonstrated the capabilities of the digital camera and rapid pulsed laser in combination with moire.

DISCUSSION

The moire methods, especially moire interferometry, has been shown to be a valuable laboratory tool in experimental mechanics of composite materials. Geometric and interferometric moire provide the experimentalist with a wide choice of in-plane displacement measurement sensitivities from 0.001" per fringe to 20 microinches per fringe thus allowing the sensitivity to be chosen to suit the experiment. For composites, the high sensitivity of moire interferometry provides numerous displacement fringes for relative low load, thus the response of the material can remain in the linear region. The areas that have been described here show the flexibility of moire methods for understanding of composite material behavior.

A major limiting factor in applying moire, other than shadow moire, is that users are restricted to the laboratory, and for interferometry a further restriction is to a vibration isolation table. Also, specimens are usually flat or only slightly curved and areas of only a few square inches are interrogated due to optics and size of gratings. Even though these factors limit the use of moire, numerous experiments have been conducted on specimens with flat surfaces under basic loading configurations as shown here and experimental results have substained elasticity solutions, worked hand-in-hand with finite element studies, and have been used to observe the response of materials under various loading configurations.

Moire experimental techniques will continue to improve in sensitivity and ease of use along with improved methods of extracting data from fringe patterns. The general application areas described here should continue with added emphasis on correlation of experimental results with finite element modeling and analysis, verification of standard test specimen configurations, interlamina and interfacial shear, and mechanical fastening experiments extended to adhesive joints. Some particular applications could be for edge examination of bolted joints, examination of crack tip in three dimension with extreme magnification and sensitivity, and measurement of dynamic events such as impact loading and crack propagation. Application of moire will continue to grow due to the demand being put on composite materials by design engineers.

REFERENCES

1. THEOCARIS, P. S. *Moire Fringes in Strain Analysis.* Pergamon Press, New York, NY, 1969.

2. DURELLI, A. J., and PARKS, V. J. *Moire Analysis of Strain.* Prentice-Hall, Inc., New York, NY, 1970.

3. CHIANG, F. P. *Moire Methods of Strain Analysis.* Manual on Experimental Stress Analysis, Society for Experimental Stress Analysis, Ch. 5, 1978.

4. PARKS, V. J. *Geometric Moire.* Society for Experimental Mechanics (SEM), Handbook on Experimental Stress Analysis, Ch. 6, A. Kobayashi, ed., 1984.

5. CHIANG, F. P. *On an Optical Moire Processor.* Theory and Technology of Moire Methods, U.S. Army Materials Technology Laboratory, AMMRC SP 80-4, 1980.

6. VOLOSHIN, A. S., BURGER, C. P., and ROWLANDS, R. E. *Composite Analysis by Fractional Moire Fringe System.* Journal of Composite Materials, v. 19, November 1985.

7. CHIANG, F. P. *First and Second Order Shadow Moire Methods.* Theory and Technology of Moire Methods, U.S. Army Materials Technology Laboratory, Ch. 10, AMMRC SP 80-4, 1980.

8. POST, D. *Developments in Moire Interferometry.* Optical Engineering, v. 21, no. 3, 1982.

9. POST, D. *High Sensitivity Moire Interferometry - A Simplified Approach.* Experimental Mechanics, v. 21, no. 3, 1981.

10. POST, D. *Moire Interferometry at VPI & SU.* Experimental Mechanics, 1983.

11. POST, D. *Optical Interferometry for Deformation Measurements - Classical, Holographic, and Moire Interferometry.* Mechanics of Nondestructive Testing, W. W. Stinchcomb, ed., Plenum Press, New York, NY, 1980.

12. POST, D. *Moire Interferometry.* Handbook on Experimental Stress Analysis, Society for Experimental Mechanics (SEM), Ch. 7, A. Kobayashi, ed., 1984.

13. BASEHORE, M. L. *High Sensitivity Moire Interferometry.* Society for Experimental Mechanics (SEM), Conference Proceedings, November 1986.

14. WEISSMAN, E. M., and POST, D. *Moire Interferometry Near the Theoretical Limit.* Applied Optics, v. 21, no. 9, May 1982.

15. HAN, B., and POST, D. *Extension of Moire Interferometry into the Ultra-High Sensitivity Domain.* Society for Experimental Mechanics (SEM), Conference Proceedings, June 1989.

16. BASEHORE, M. L. *High-Frequency, High-Reflectance Transferable Moire Gratings.* Experimental Techniques, May 1984.

17. ANASTASI, R. F., DAI, Y. Z, and CHIANG, F. P. *Simplified Procedures for Obtaining High-Frequency Highly-Reflective Specimen Gratings for Moire Interferometry.* Experimental Techniques, September 1988.

18. GUO, Y., POST, D., and CZARNEK, R. *The Magic of Carrier Patterns in Moire Interferometry.* Society of Photo-Optical Instrumentation Engineers (SPIE), Conference on Photomechanics and Speckle Metrology, v. 814, 1987.

19. RANSON, W. F. *Computer Vision Equipment in the Mechanics Laboratory.* Society for Experimental Mechanics (SEM), Conference Proceedings, June 1986.

20. SCIAMMARELLA, C. A., and AHMADSHAHI, M. *An Opto-Electronic System for Fringe Pattern Analysis.* Experimental Techniques, 1986.

21. CHOUDRY, A. *Automated Fringe Reduction Techniques.* Society of Photo-Optical Instrumentation Engineers (SPIE), v. 816, 1987.

22. NING, P. T., and PENG, W. L. *Automated Analysis of Moire Fringe Patterns by Using an Image Processing System.* Experimental Mechanics, v. 28, no. 4, December 1988.

23. LEE, C. A., RICHARD, T. G., and ROWLANDS, R. E. *Exact Interpretation of Moire Fringe Patterns in Digital Images.* Experimental Mechanics, v. 28, no. 4, December 1988.

24. OPLINGER, D. *Computerized Analysis of Moire Patterns.* Society for Experimental Stress Analysis (SESA), June 1982.

25. SEGALMAN, D. B., WOYAK, D. B., and ROWLANDS, R. E. *Smooth Spline-Like Finite Element Differentiation of Full-Field Experimental Data Over Arbitrary Geometry.* Experimental Mechanics, December 1979.

26. TESSLER, A., FREESE, C., ANASTASI, R. F., SERABIAN, S. M., OPLINGER, D. W., and KATZ, A. *Least Squares Penalty Constraint Finite Element Method for Generating Strain Fields from Moire Patterns.* Society of Photo-Optical Instrumentation Engineers (SPIE), v. 814, 1987.

27. GILBERT, J. A. *Two-Dimensional Stress Analysis Combining High-Frequency Moire Measurements with Finite Element Modeling.* Experimental Techniques, March 1987.

28. GRIMES, G. C., and REIMANN, L. F. *Analysis of Discontinuities, Edge Effects, and Joints.* Structural Design and Analysis, Part II, Ch. 10, C. C. Chamis, ed., Academic Press, San Diego, CA, 1974.

29. HALPIN, J. C. *Primer on Composite Materials Analysis.* Technomic Publishing Co., Inc., Lancaster, PA, 1984.

30. JONES, R. M. *Mechanics of Composite Materials.* Hemisphere Publishing Corp., New York, 1975.

31. TSAI, S. W. *Introduction to Composite Materials.* Technomic Publishing Co., Inc., Lancaster, PA, 1980.

32. TSAI, S. W. *Composite Design 1986.* Think Composites, Dayton, OH, 1986.

33. PIPES, R. B., and DANIEL, I. M. *Moire Analysis of the Interlaminar Shear Effect in Laminated Composites.* Journal of Composites, v. 5, April 1971.

34. OPLINGER, D. W., PARKER, B. S., and CHIANG, F. P. *Edge-Effect Studies in Fiber-Reinforced Laminates.* Experimental Mechanics, September 1974.

35. OPLINGER D. W. *Applications of Moire Methods to Evaluation of Structural Performance of Composite Materials.* Optical Engineering, v. 21, no. 4, July/August 1982.

36. CZARNEK, R., POST, D., and HERAKOVICH, C. T. *Edge Effects in Composites by Moire Interferometry.* Experimental Techniques, January 1983.

37. HERAKOVICH, C. T., and POST, D. *Free Edge Strain Concentrations in Real Composite Laminates: Experimental-Theoretical Correlation.* Journal of Applied Mechanics, v. 57, December 1985.

38. PIPES, R. B., and PAGANO, J. J. *Interlaminar Stresses in Composite Laminates Under Axial Extension.* Journal of Composite Material, no. 4, 1970.

39. IFJU, P., and POST, D. *Thermal Strain Analysis Using Moire Interferometry.* Society of Photo-Optical Instrumentation Engineers (SPIE), v. 814, 1987.

40. WANG, Y., DAI, F., and POST, D. *Interlaminar Compression of a Thick Composite.* Society for Experimental Mechanics (SEM), Conference Proceedings, June 1989.

41. BOEMAN, R., CZARNEK, R., and POST, D. *Interlaminar Deformations on the Boundary Surface of a Hole in a Thick Composite.* Society for Experimental Mechanics (SEM), Conference Proceedings, June 1989.

42. McDONACH, A., McKELVIE, J., MacKENZIE, P., and WALKER, C. A. *Improved Moire Interferometry and Applications in Fracture Mechanics, Residual Stress, and Damaged Composites.* Experimental Techniques, June 1983.

43. WOOD, J. D. *Detection of Delamination Onset in a Composite Laminate Using Moire Interferometry.* Journal of Composite Technology and Research, v. 7, no. 4, 1985.

44. MOUSLEY, R. F. *A Shadow Moire Technique for the Measurement of Damage in Composites.* Composite Structures, no. 4, 1985.

45. JONES, R., BOUGHTON, W., MOUSLEY, R. F., and POTTER, R. T. *Compression Failure of Damaged Graphite Epoxy Laminates.* Composite Structures, no. 3, 1985.

46. SCHWARZ, R. C. *Determination of Out-of-Plane Displacements and the Initiation of Buckling in Composite Structural Elements.* Experimental Techniques, January 1988.

47. DANIEL, I. M., and ROWLANDS, R. E. *Determination of Strain Concentration in Composites by Moire Techniques.* Journal of Composite Materials, v. 5, 1971.

48. DANIEL, I. M., ROWLANDS, R. E., and POST, D. *Strain Analysis of Composites by Moire Methods.* Experimental Mechanics, June 1973.

49. POST, D. *Observations of Elastic-Plastic Displacement Fields Around Cracks by Moire Interferometry.* Society for Experimental Stress Analysis (SESA), Conference Proceedings, June 1984.

50. ASUNDI, A., and HEUNG, M. T. *Developments in Moire Interferometry for Out-of-Plane Displacement Measurement.* Society for Photo-Optical Instrumentation Engineers (SPIE), v. 814, 1987.

51. POST, D., CZARNEK, R., JON, D., and GUO, Y. *Experimental Study of a Metal Matrix Composite.* Society for Experimental Mechanics (SEM), Conference Proceedings, June 1986.

52. POST, D., CZARNEK, R., and JON, D. *Shear Strains in Graphite-Peek Beam by Moire Interferometry with Carrier Fringes.* Experimental Mechanics, v. 27, 1987.

53. POST, D., CZARNEK, R., JON, D., and WOOD, J. *Shear Strain Anomalies in Composite Beam Specimens by Moire Interferometry.* Society for Experimental Mechanics (SEM), Conference Proceedings, June 1985.

54. POST, D., CZARNEK, R., JON, D., and WOOD, J. *Deformation of Composite Multi-Span Beam Shear Specimens.* Society for Experimental Mechanics (SEM), Conference Proceedings, June 1984.

55. POST, D., GUO, Y., and IFJU, P. *Interlaminar Shear Moduli of Cross-Ply Laminates: An Experimental Analysis.* Journal of Composite Materials, v. 23, March 1989.

56. ABDALLAH, M. G., GARDINER, D. S., and GASCOIGNE, H. E. *An Evaluation of Graphite/Epoxy Iosipescu Shear Specimen Testing Methods with Optical Techniques.* Society for Experimental Mechanics (SEM), Conference Proceedings, June 1985.

57. IFJU, P., and POST, D. *A Compact Double Notched Specimen for In-Plane Shear Testing.* Society for Experimental Mechanics (SEM), Conference Proceedings, June 1989.

58. PINDERA, M., IFJU, P., and POST, D. *Iosipescu Shear Charterization of Polymeric and Metal Matrix Composite.* Society for Experimental Mechanics (SEM), Conference Proceedings, June 1989.

59. OPLINGER, D. W. *On the Structural Behavior of Mechanically Fastened Joints in Composites.* Fibrous Composites in Structural Design, Leno, Burk, and Oplinger, eds., Plenum Press, New York, NY, 1980.

60. KOSHIDE, S. *Investigation of Pin Joints in Composites by the Moire Method.* Experimental Mechanics, v. 26, no. 2, June 1986.

61. SERABIAN, S. M., and OPLINGER, D. W. *An Experimental and Finite Element Investigation into the Mechanical Response of 0/90 Pin-Loaded Laminates.* Journal of Composite Material, v. 21, July 1987.

62. TSAI, M. Y., HAN, B., MORTON, J., and POST, D. *Contact Stress in Pin-Loaded Plates - An Experimental Study.* Society for Experimental Mechanics (SEM), Conference Proceedings, June 1989.

63. HERRERA-FRANCO, P. J., and CLOUD, G. *Moire Study of Mechanically Fastened Composite*. Society for Experimental Mechanics (SEM), Conference Proceedings, June 1985.

64. HERRERA-FRANCO, P. J., and CLOUD, G. *Experimental Analysis of Multiple-Hole Arrays of Composite Material Fasteners*. Society for Experimental Mechanics (SEM), Conference Proceedings, June 1986.

65. BAYER, M. H., and CLOUD, G. *Moire Study of Strains Near Washers on Composites*. Society for Experimental Mechanics (SEM), Conference Proceedings, November 1986.

66. CLOUD, G., HERRERA-FRANCO, P. J., and BAYER, M. H. *Some Strategies to Reduce Stress Concentrations at Bolted Joints in FGRP*. Society for Experimental Mechanics (SEM), Conference Proceedings, June 1989.

67. LEE, J., CZARNEK, R., and GUO, Y. *Interferometric Study of Residual Strain in Thick Composites*. Society for Experimental Mechanics (SEM), Conference Proceedings, June 1989.

68. MORTON, J., and POST, D. *Applications of Photomechanics to the Study of Solid Mechanics Phenomena and Material Property Measurement*. U.S. Army Symposium on Solid Mechanics, U.S. Army Materials Technology Laboratory, April 1989.

69. CZARNEK, R., POST, D., and GUO, Y. *Non-Uniformity in Composite Panels by Moire Interferometry*. Society of Experimental Mechanics (SEM), Conference Proceedings, June 1986.

70. ARMENAKAS, A. E., and SCIAMMARELLA, C. A. *Response of Glass-Fiber-Reinforced Epoxy Specimens to High Rates of Tensile Loading*. Experimental Mechanics, October 1973.

71. EPSTEIN, J. S., DEASON, V. A., and ABDALLAH, M. *Studies of Stress Wave Propagation in Composites*. Society of Experimental Mechanics (SEM), Conference Proceedings, November 1986.

72. DEASON, V. A., and EPSTEIN, J. S. *Interfacial Shear Phenomena in Graphite Epoxy Composites Under Impact Loading Using Dynamic Moire Interferometry*. Society of Photo-Optical Instrumentation Engineers (SPIE), v. 814, 1987.

73. HSU, T. Y., LIU, B. C., CHIANG, F. P., and ANASTASI, R. F. *Study of Loading Rate Effect on Composites Using a High Speed Digital Camera*. Society for Experimental Mechanics (SEM), Conference Proceedings, June 1989.

74. WALKER, C. A., and McKELVI, J. *Optical Methods*. Non-Destructive Testing of Fiber Reinforced Plastic Composites, Ch. 4, J. Summerscales, ed., Elsever Applied Science Publishers, LTD, New York, 1987.

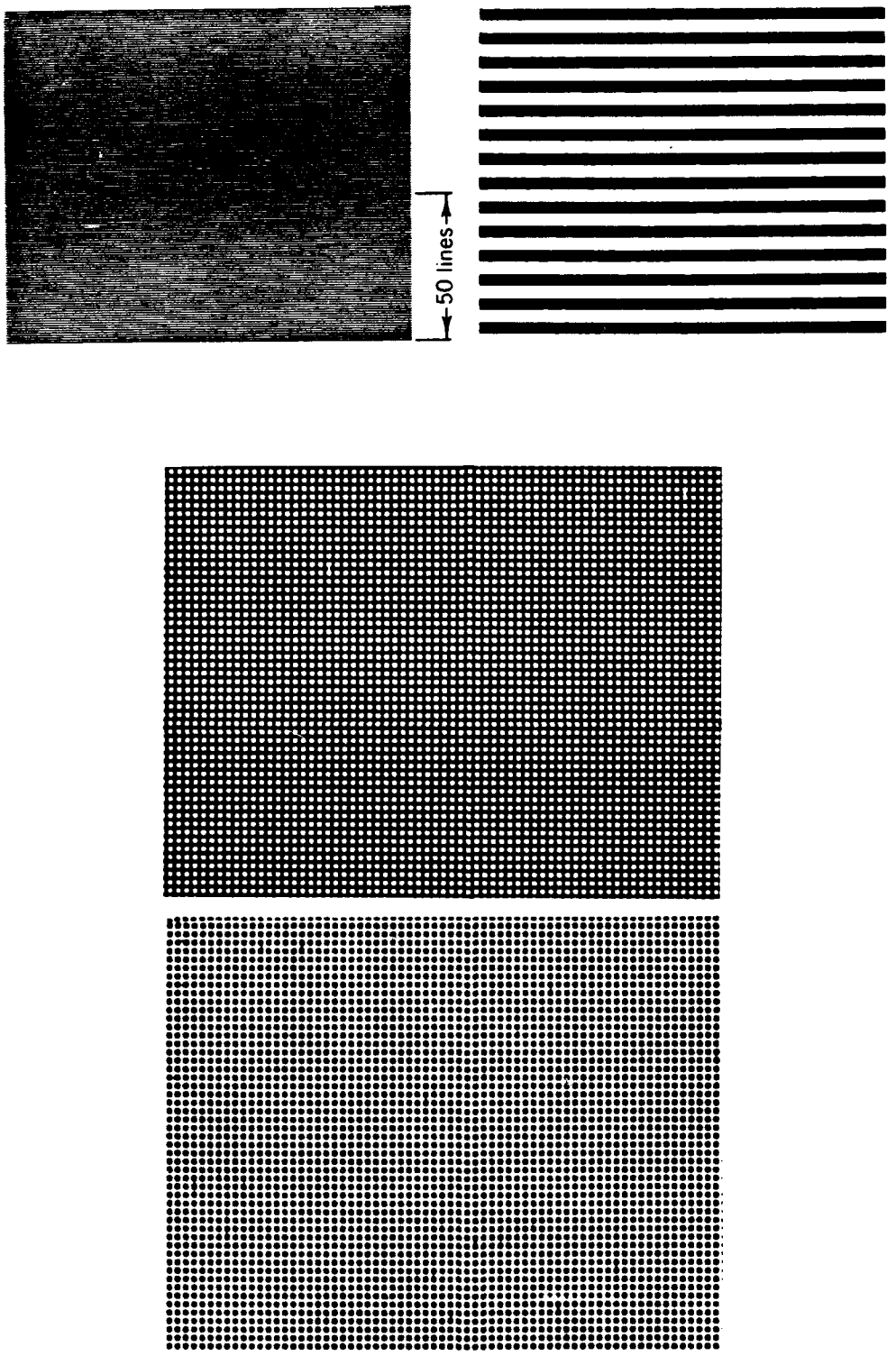

Figure 1. Typical gratings of straight parallel lines (top), crossed lines (center), and dots in square array (bottom), (Ref. 2).

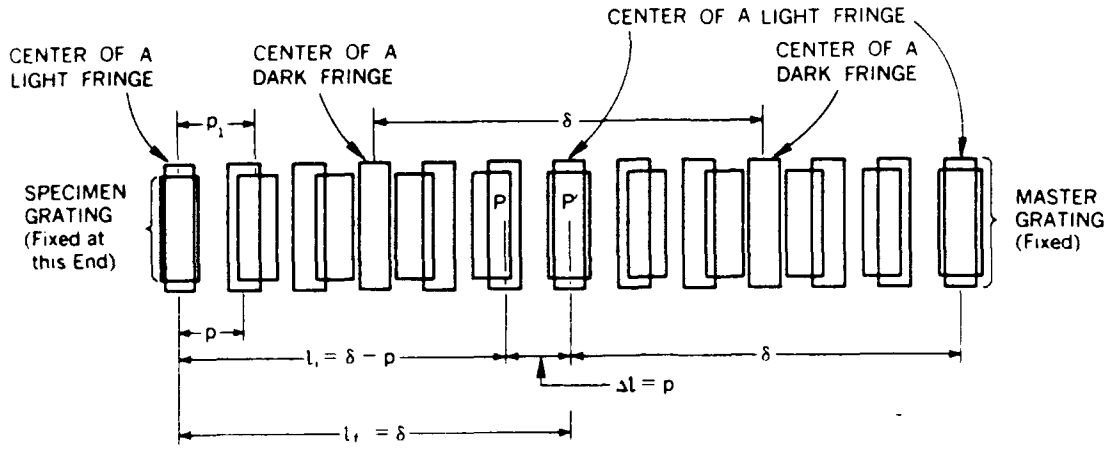

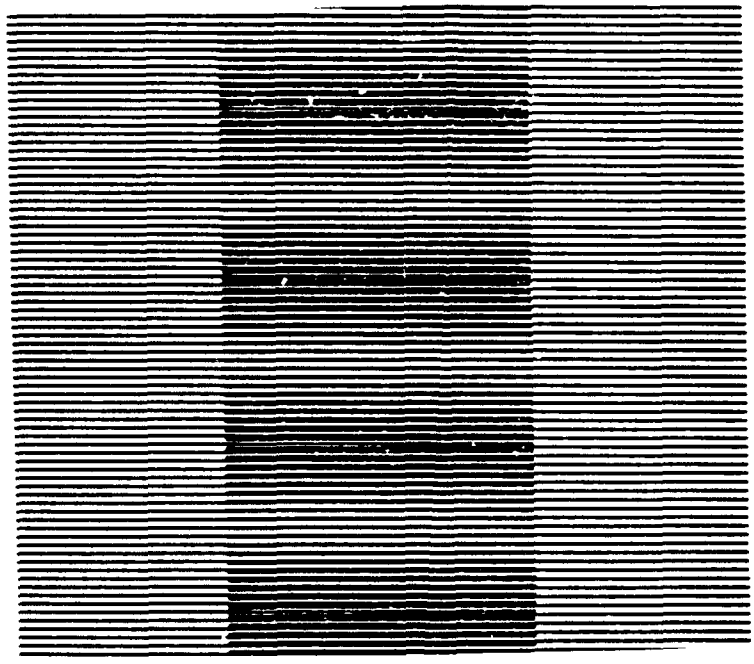

Figure 2. Formation of moire fringes without relative rotation of the grating (top, Ref. 2), and moire fringes formed by parallel gratings of slightly different pitch, (bottom, Ref. 1).

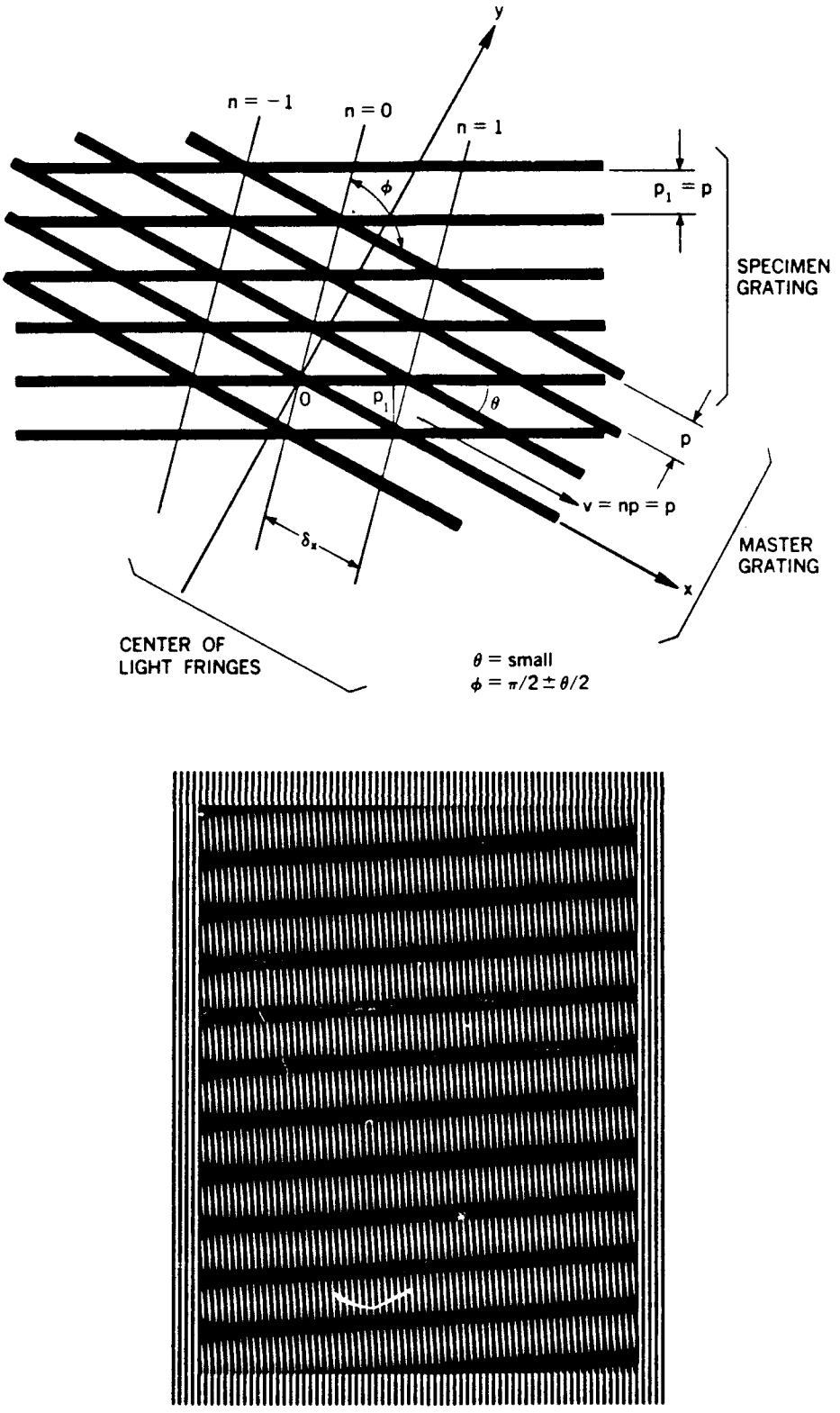

Figure 3. Moire fringes produced by pure rotation, schematic (top, Ref. 3), and real pattern (bottom, Ref. 1).

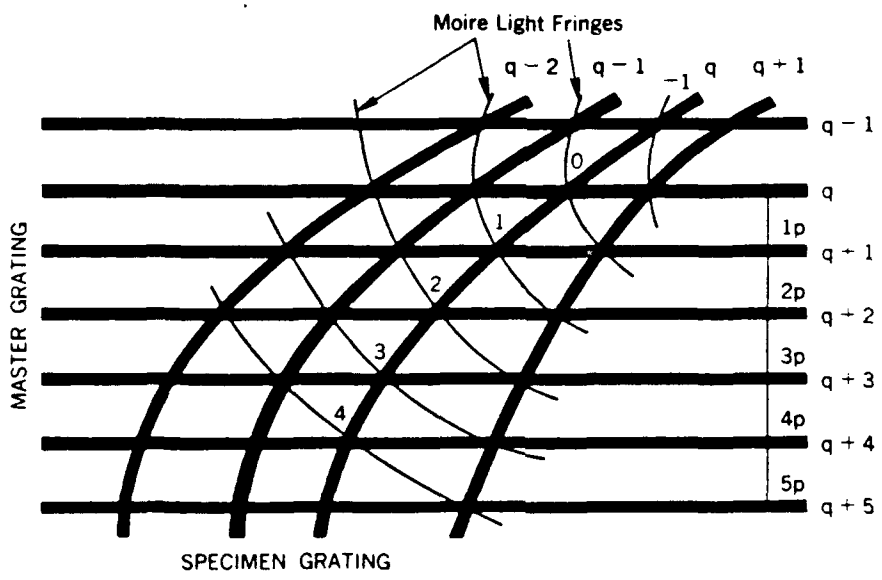

Figure 4. Moire fringes (schematic) produced by combination of pitch change and rotation, (Ref. 1).

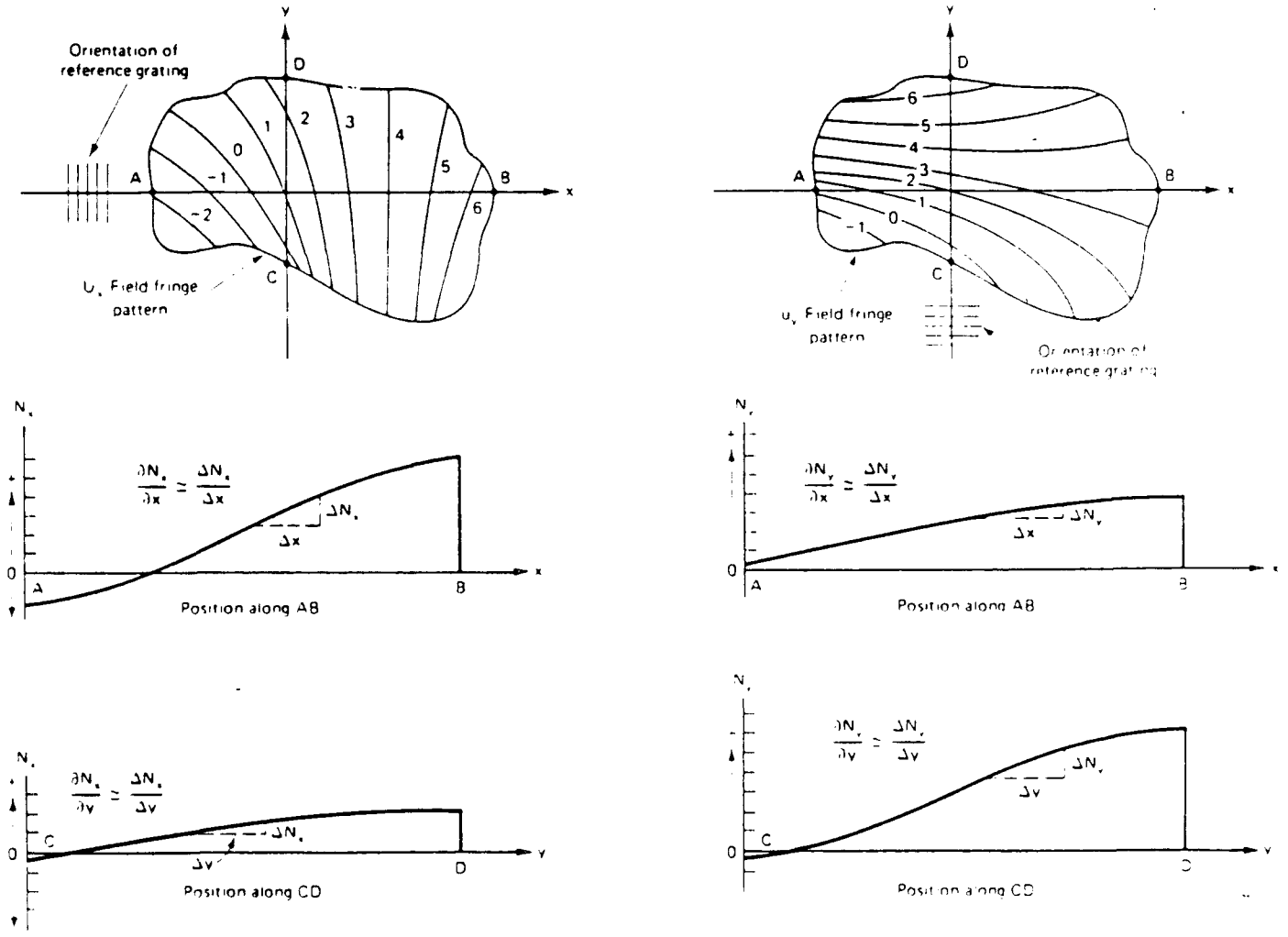

Figure 5. Illustration of procedure to obtain the four Cartesian fringe derivatives from the two Cartesian fringe patterns, (Ref. 4).

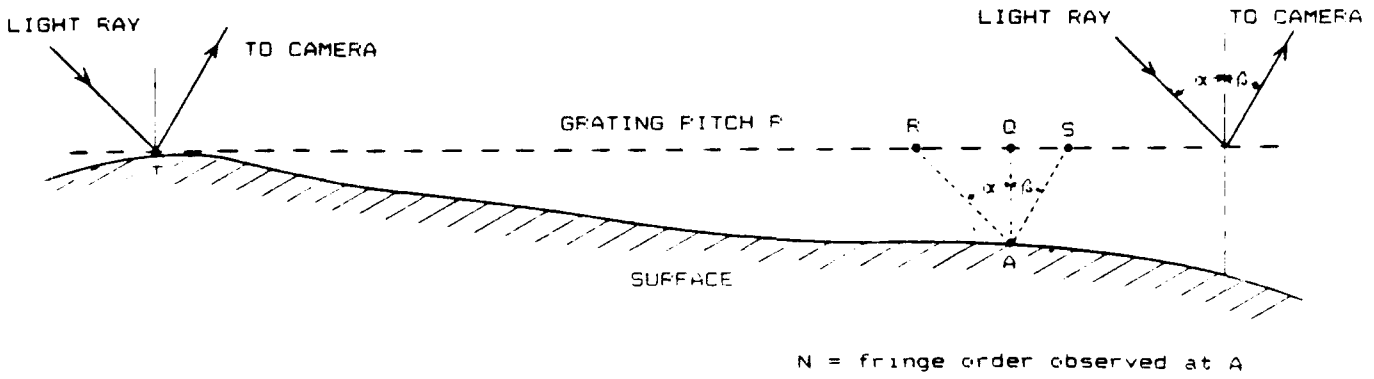

$$W = \frac{N\,P}{TAN(\alpha) + TAN(\beta)} \quad \text{inches}$$

Figure 6. Schematic of shadow moire method with parallel illumination and parallel receiving, (Ref. 3).

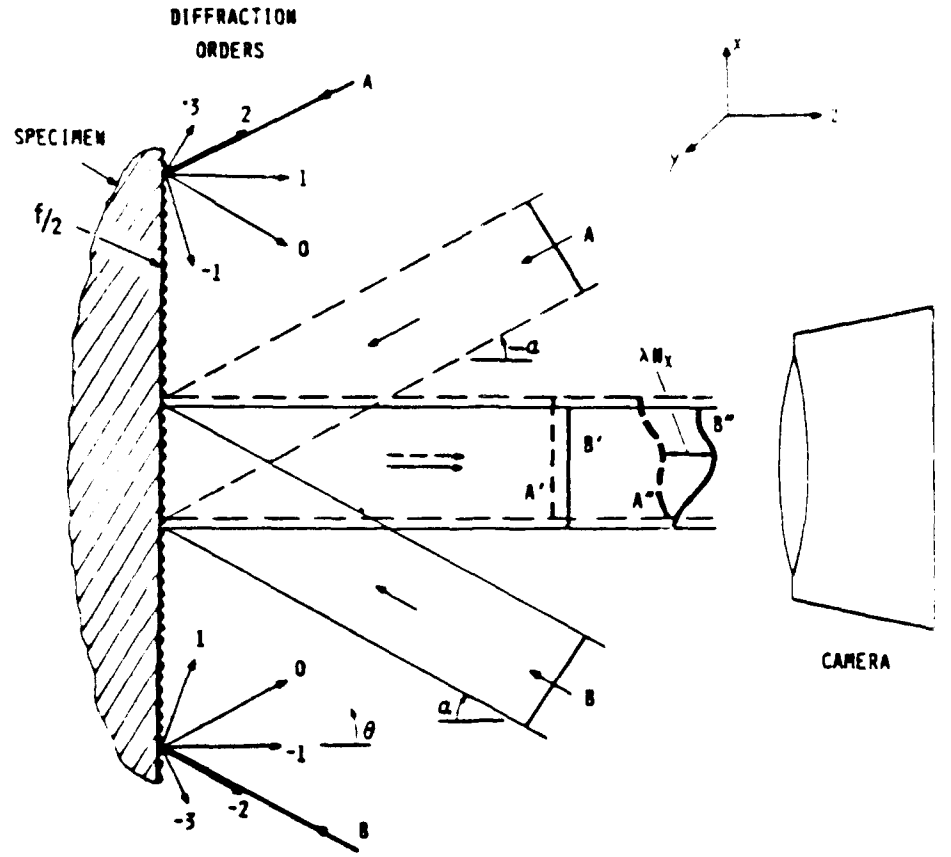

Figure 7. Basic scheme of moire interferometry, (Ref. 8).

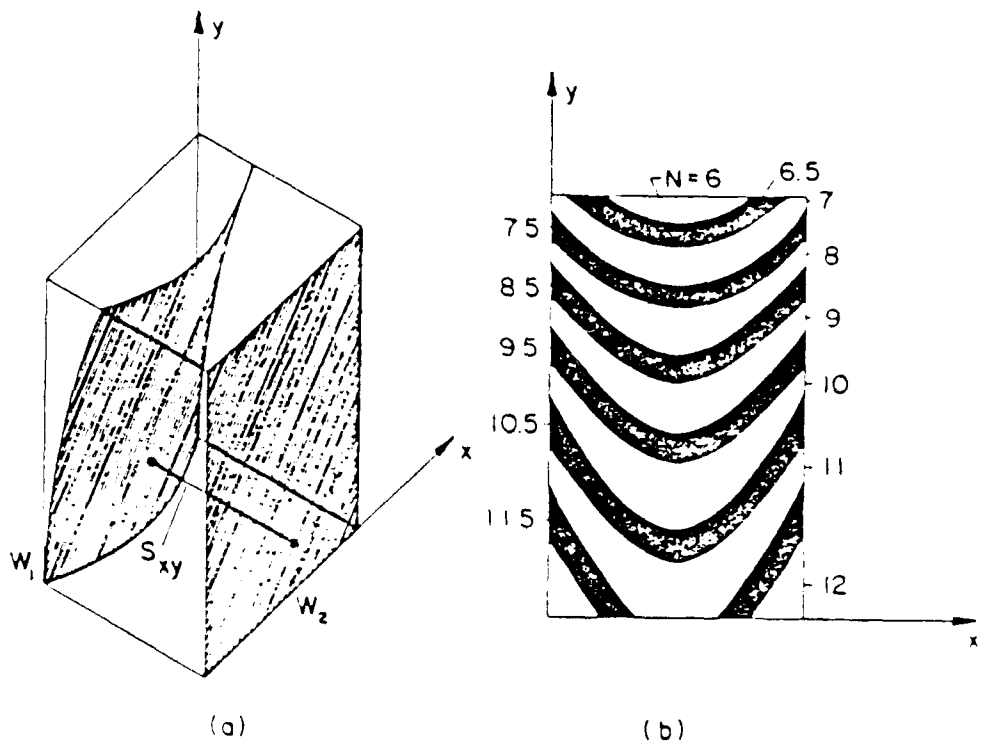

Figure 8. Two interferring wave fronts (W1 and W2), produce interference fringes, (Ref. 12).

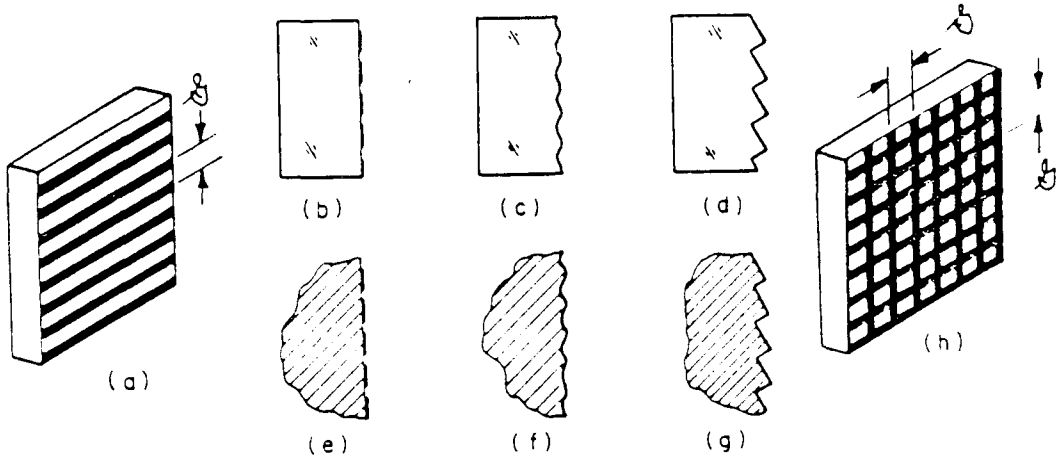

Figure 9. Diffraction gratings are comprised of regularly spaced bans or furrows. Cross-sectioned views (b), (c), and (d) illustrate transmission gratings, while (e), (f), and (g) illustrate reflection gratings; (b) and (e) represent bar and space gratings called amplitude gratings; (c) and (f) represent symmetrical phase gratings; (a) and (g) represent blaze phase gratings; (h) illustrates a cross-lined grating, which can be either amplitude or phase type, (Ref. 12).

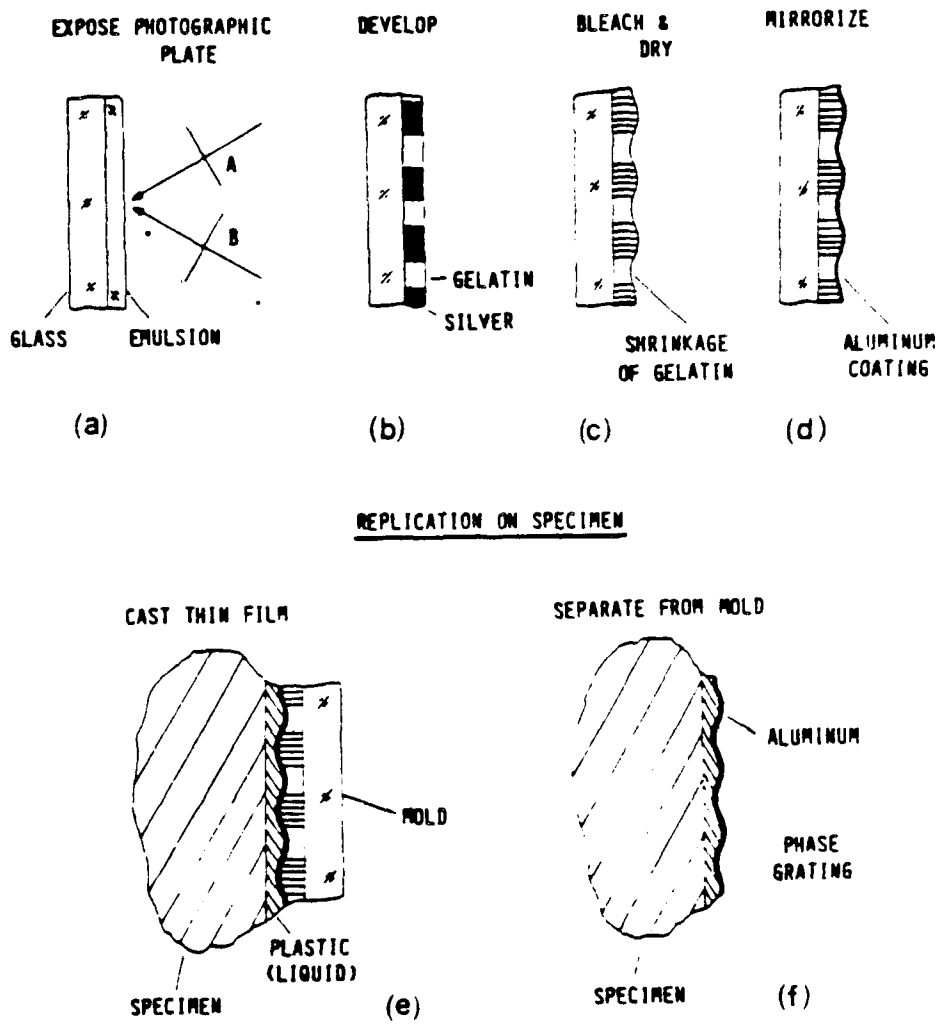

Figure 10. Steps in forming the specimen grating, (Ref. 8).

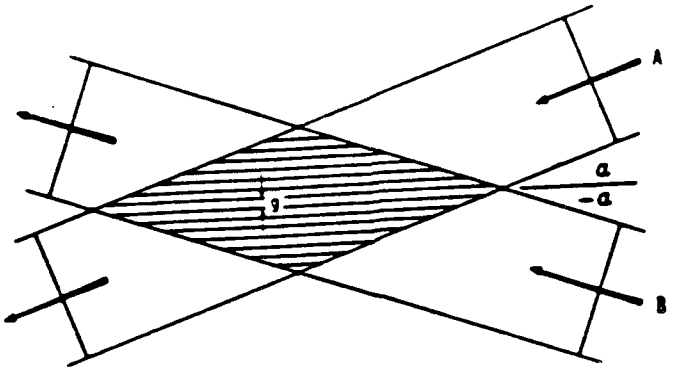

Figure 11. Intersection of two mutually coherent beams produce a virtual grating of pitch g, (Ref. 8).

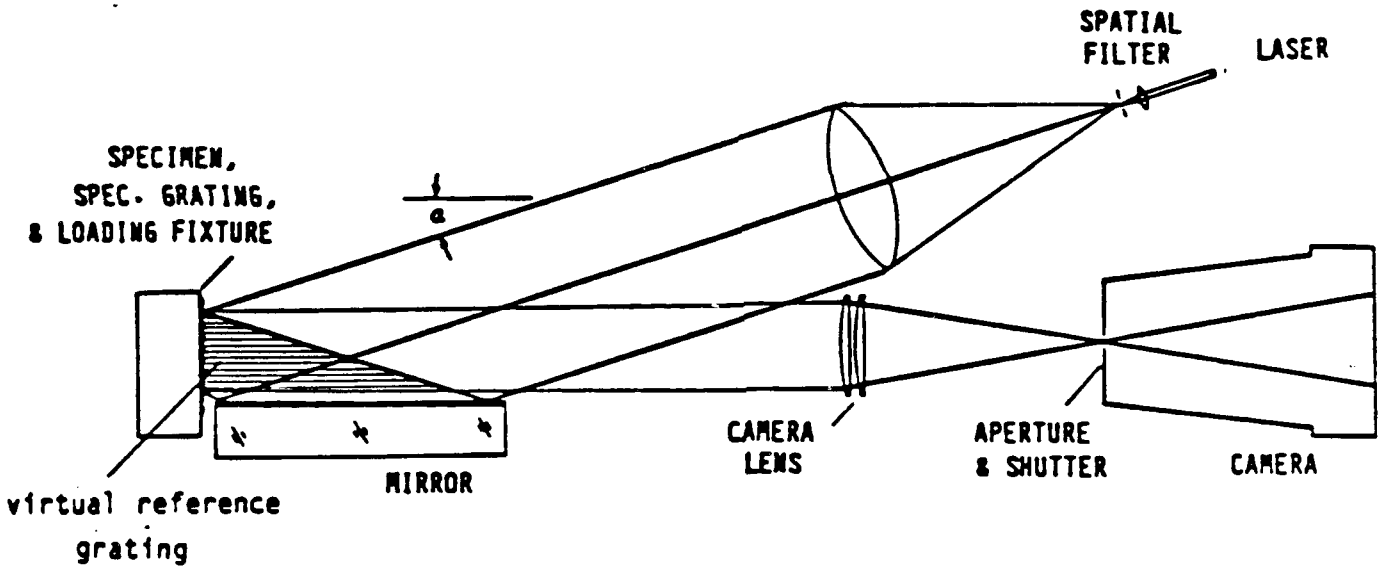

Figure 12. Moire interferometry optical arrangement using a plane mirror to form the virtual reference grating, (Ref. 8).

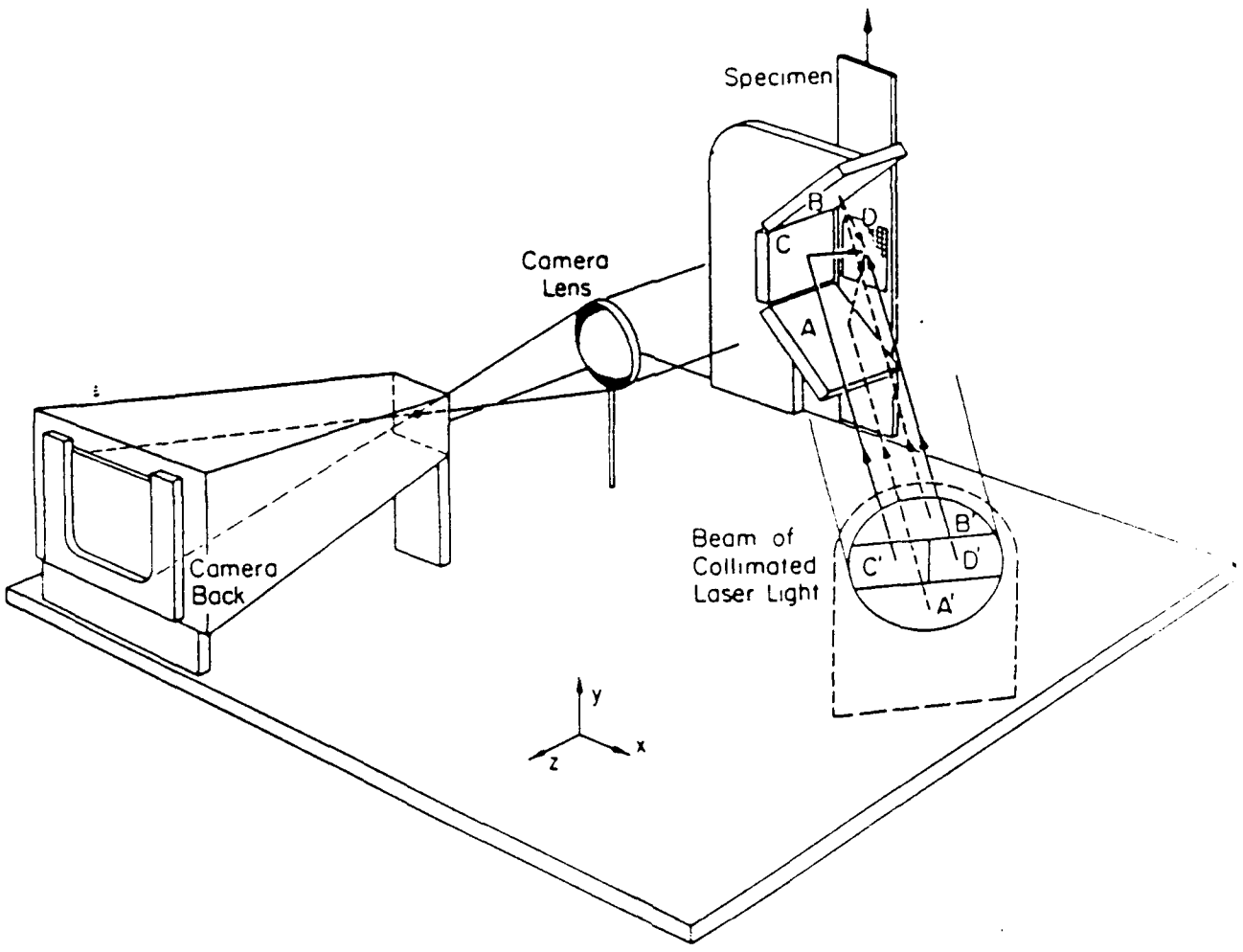

Figure 13. Four beam optical arrangement to produce the Nx pattern with beams C' and D' and the Ny pattern with beams A' and B', (Ref. 12).

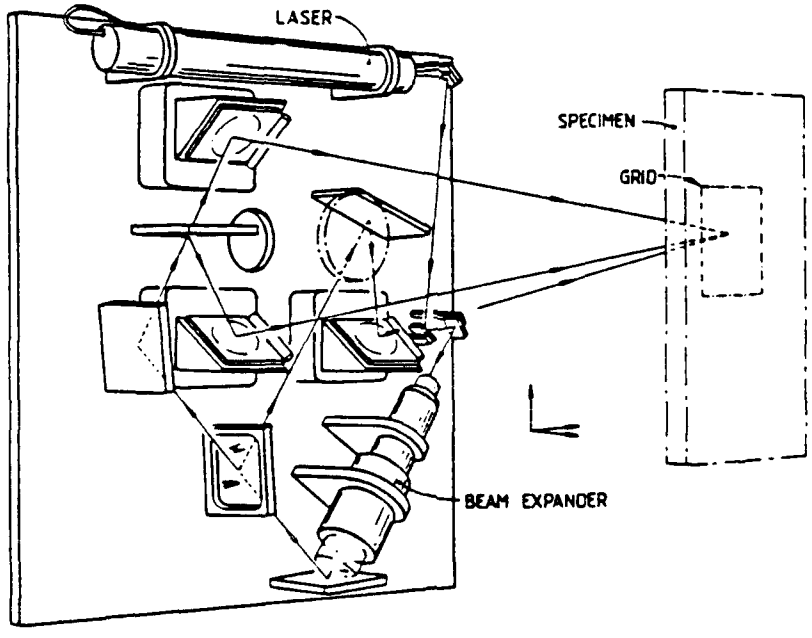

Figure 14. Folded three beam optical arrangement (Ref. 74).

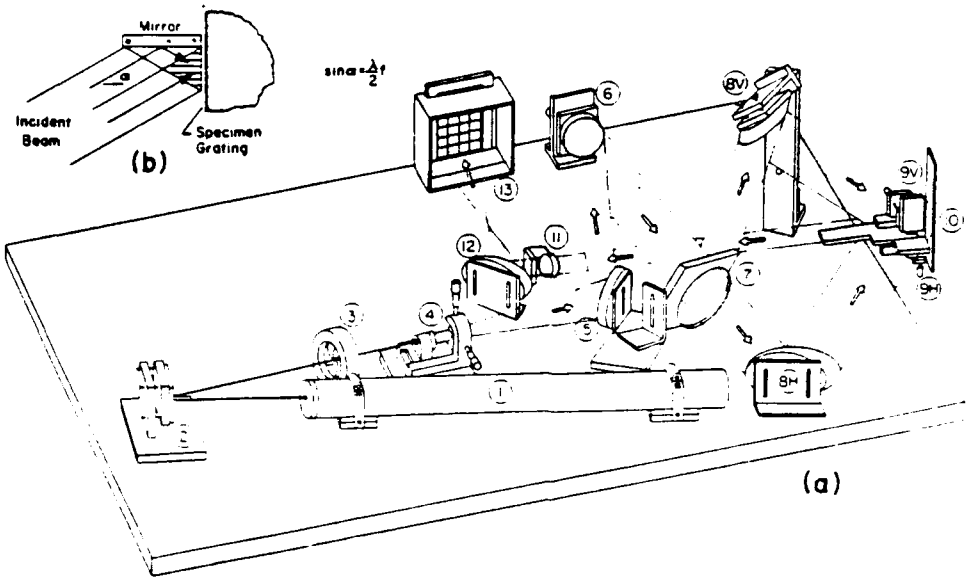

Figure 15. (a) Optical arrangement and (b) formation of virtual reference grating: (1) HeNe laser, (2,5,8,9,12) plane mirror, (3) camera shutter, (4) beam expander, (6) parabolic mirror, (7) beam splitter, (10) specimen grating, (11) collimating lens, and (13) film plane, (Ref. 43).

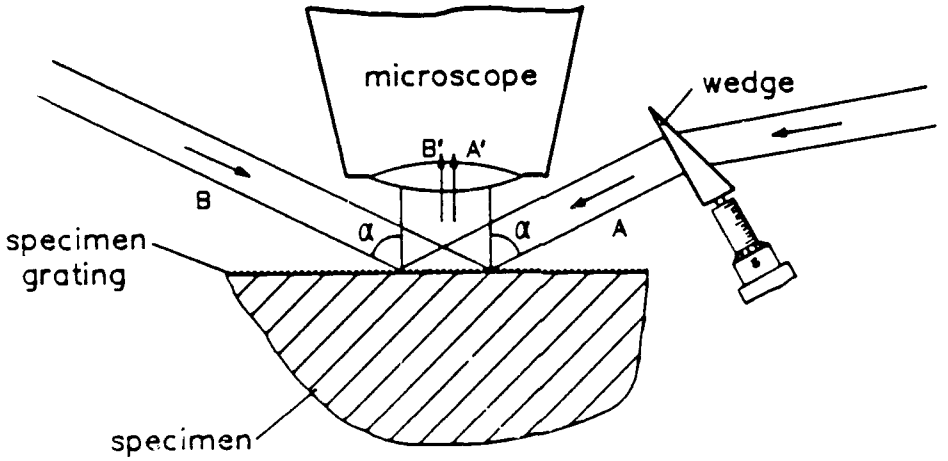

Figure 16. Proposed optical arrangement, with shallow wedge for ultra-high frequency moire, (Ref. 15).

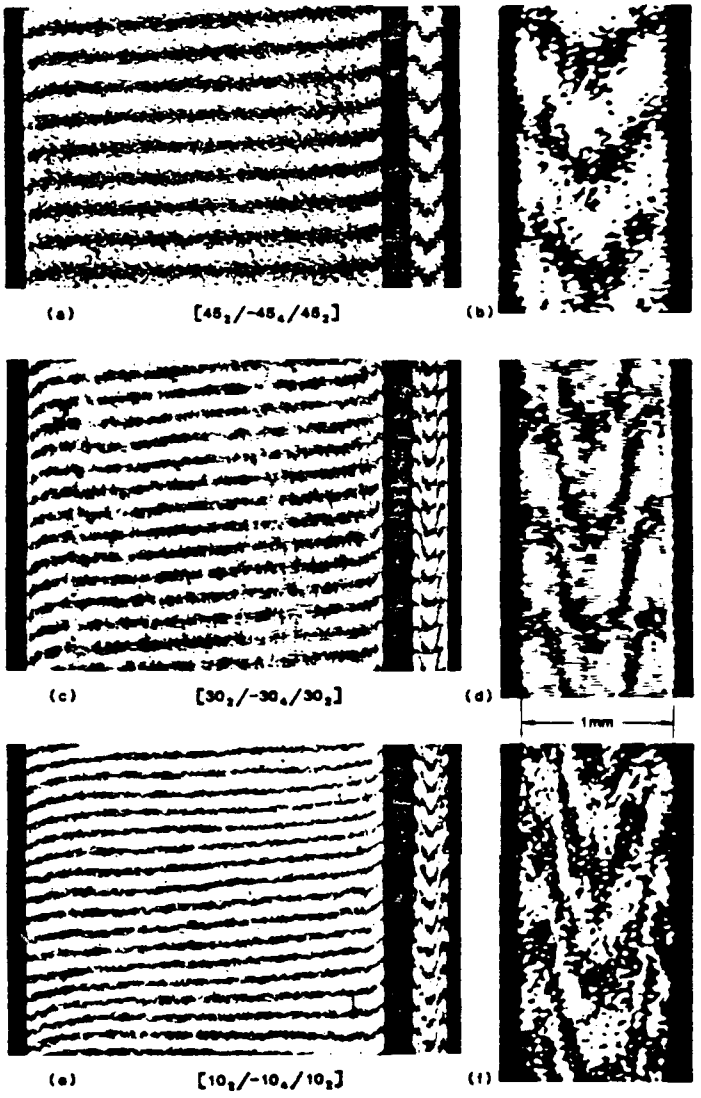

Figure 17. Magnified view of fringe patterns for specimen face and edge. Axial strain is greater in (b) than (a); it is equal in (c) and (d) and also in (e), (Ref. 36).

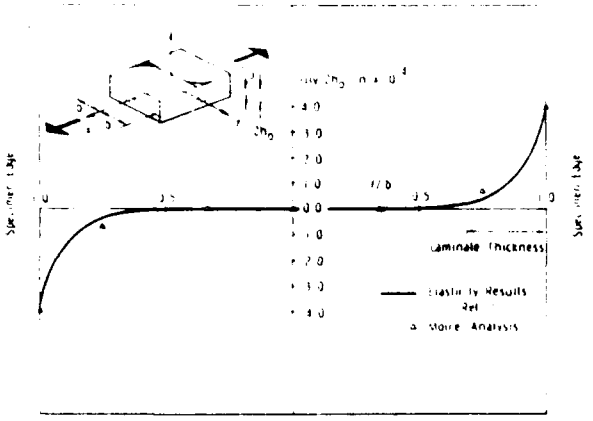

(A)

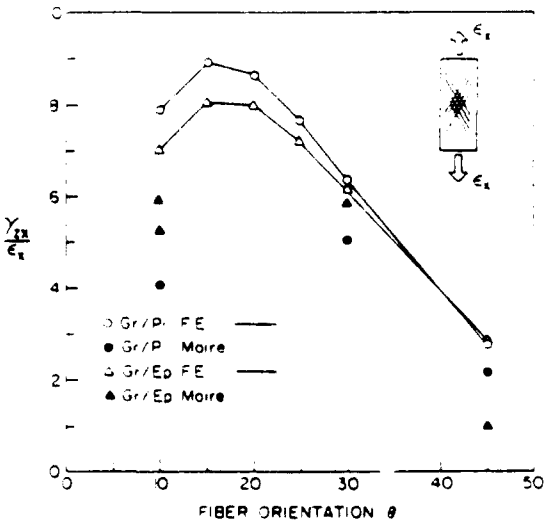

(B)

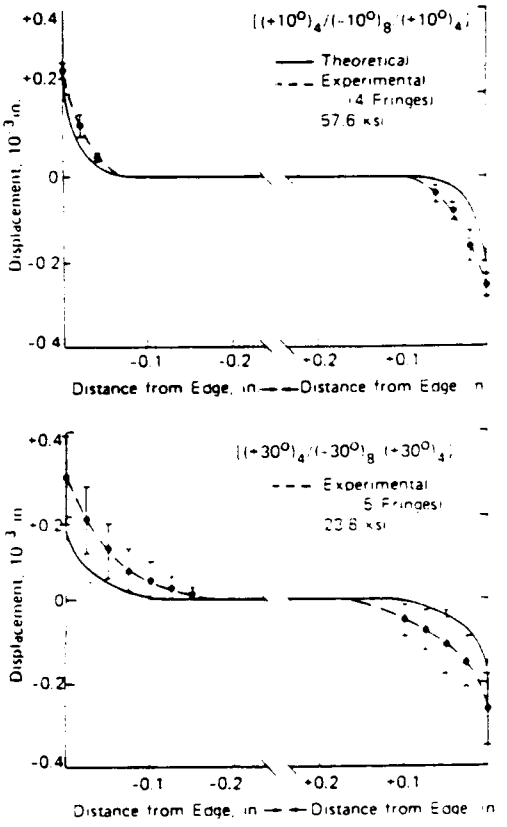

(C)

Figure 18. Experimental/Theoretical comparison. (A) Axial displacement distribution at the laminate surface $z=2h_0$, (Ref. 33). (B) Moire/Finite Element correlation for maximum strain concentrations on free edges, (Ref. 37). (C) Moire/Theoretical comparison of front face shear displacements, (Ref. 34).

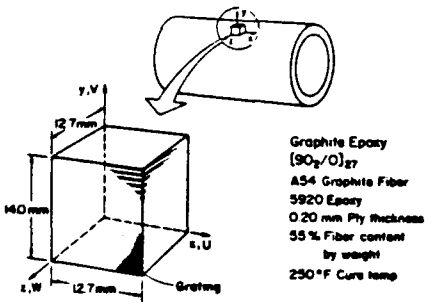

(a)

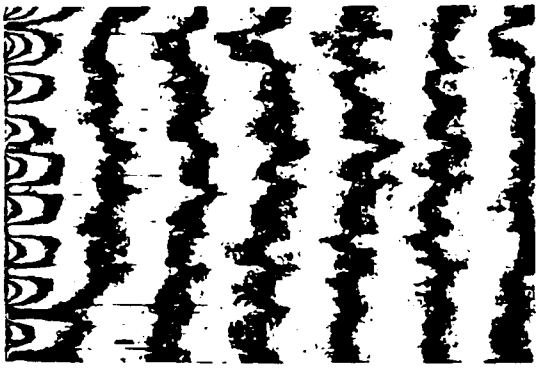

(b)

Figure 19. Edge effects on a thick walled specimen, cylinder and specimen specifications (top), and U-displacement fields (center and bottom), (Ref. 39).

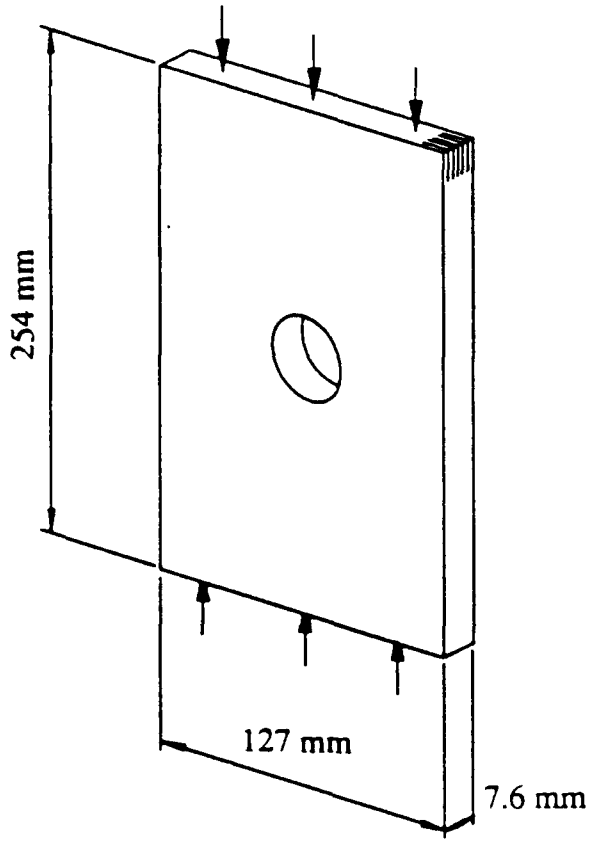

Stacking Sequence

$[0_2/90]_{5S}$

$[0/45/90/-45/0]_{3S}$

Hole Size

2.54 mm Dia. Circle
2.54 x 38.1 mm Ellipse

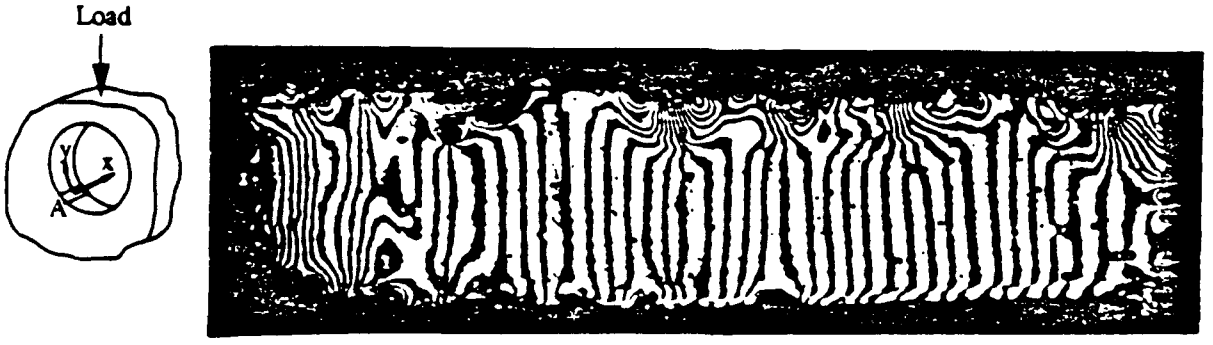

Figure 20. Moire interferometry on an internal free edge, specimen geometry and loading (top), and fringe pattern of the axial (x) displacement in the region A, for a load of 60kN (bottom), (Ref. 41).

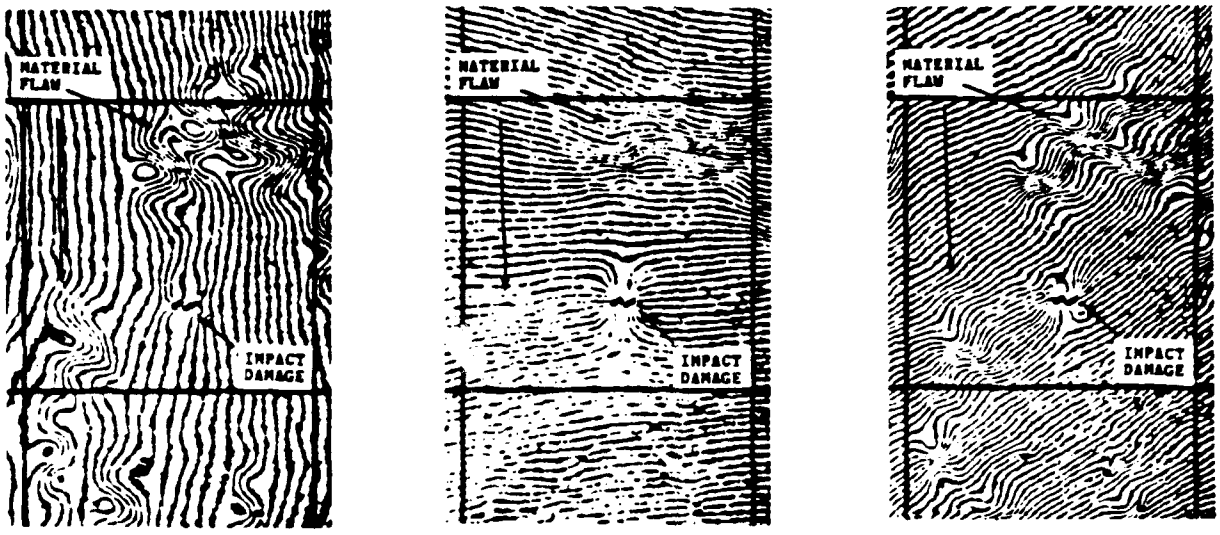

Figure 21a. Displacement concentrations due to impact damage and cyclic load, x-direction, y-direction, and 45-deg. direction (left, center, and right respectively), (Ref. 43).

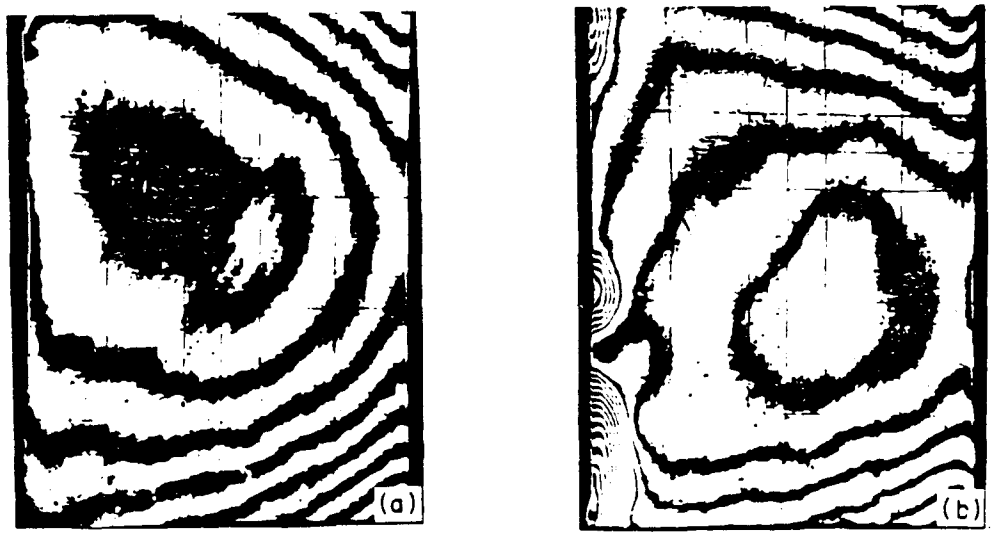

Figure 21b. Damage onset; before damage (left) and after damage (right), (Ref. 43).

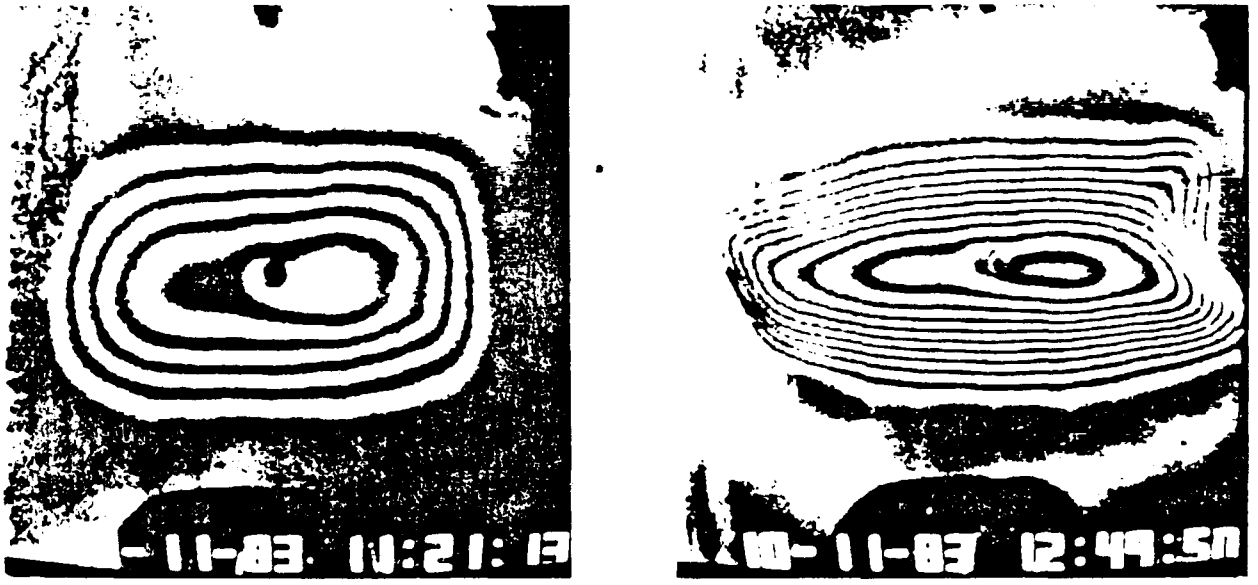

Figure 22. Buckling deformation recorded by shadow moire 25kN load (left), and delamination growth (right) at 83.9 kN load, (Ref. 45).

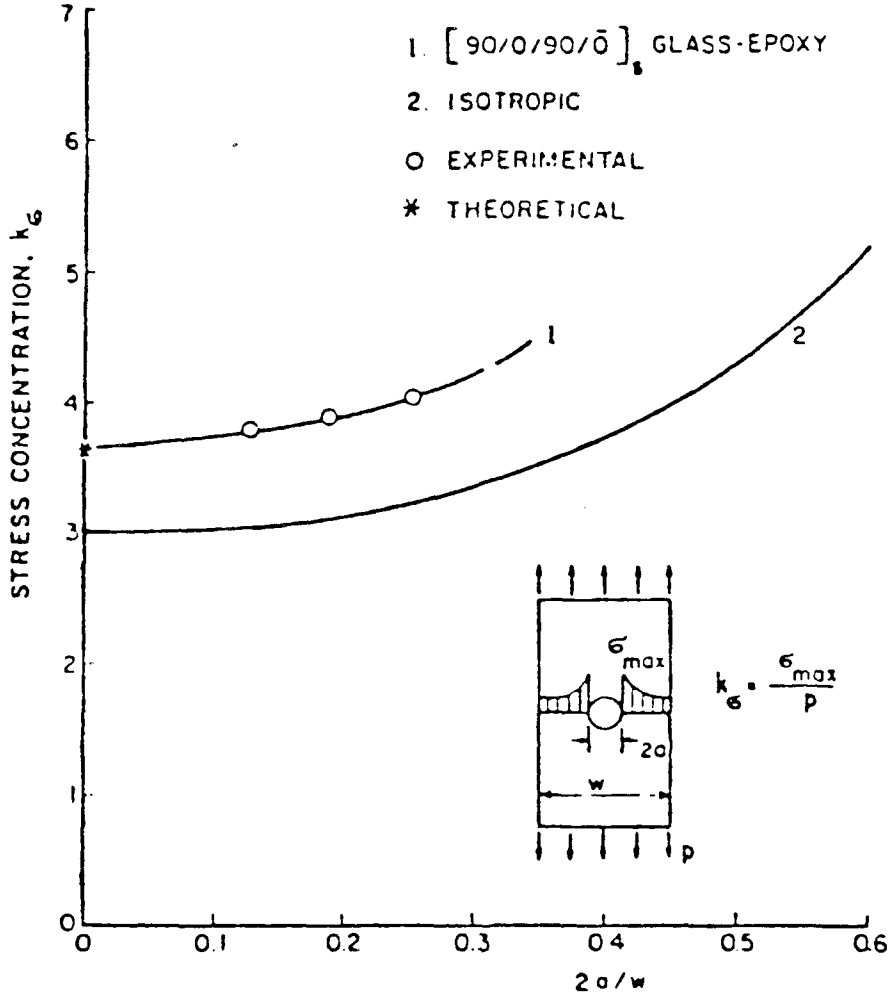

Figure 23. Stress concentration factor as a function of hole diameter to width ration, (Ref. 47).

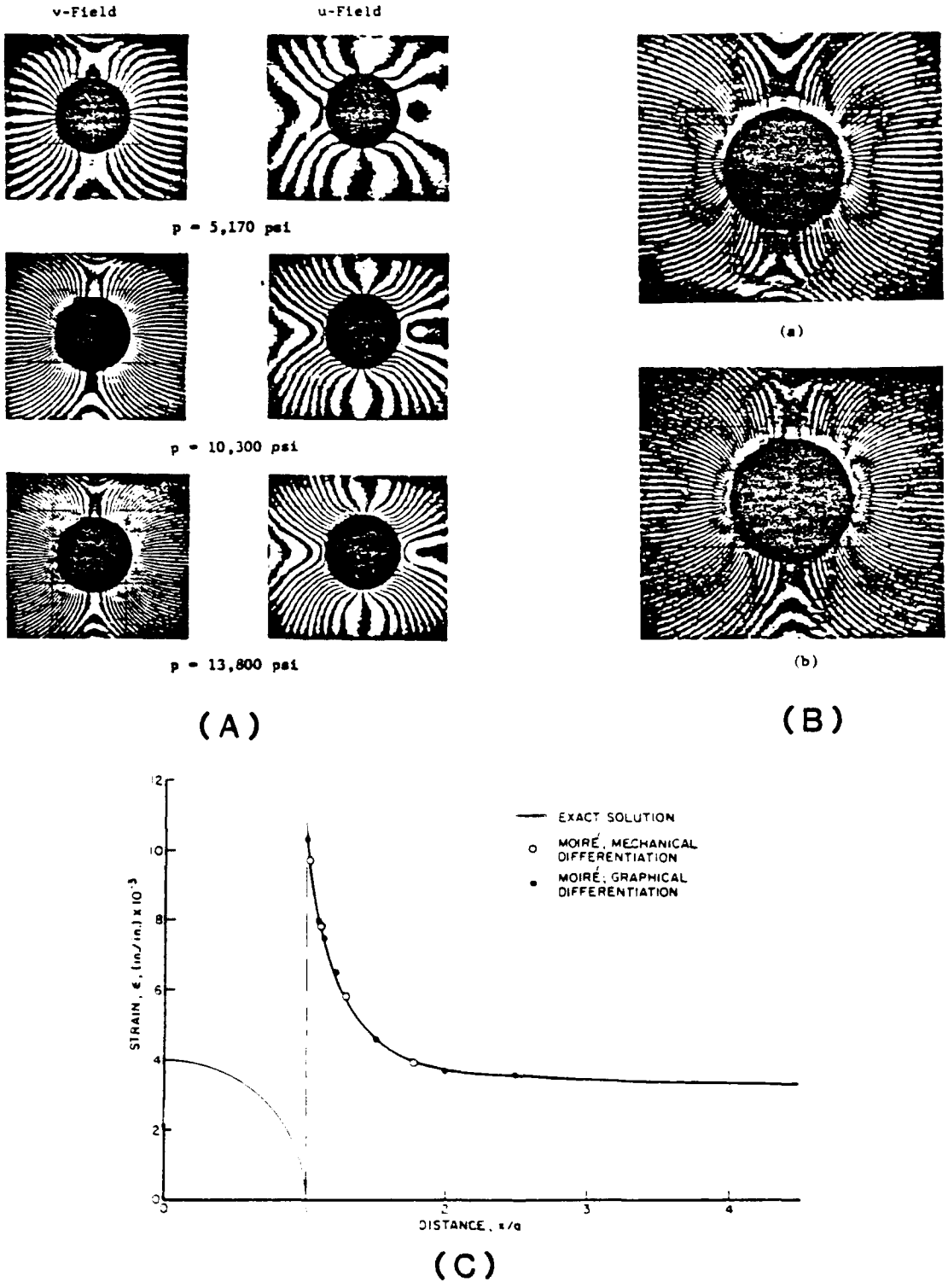

Figure 24. Experimental/Theoretical comparison of strain distribution in a plate with a hole, (Ref. 48), (A) Moire fringe pattern, glass/epoxy specimen, (B) Mechanical differentiation of moire fringe patterns,

(a) dV/dY at p=11, 950 psi

(b) dV/dy at p=13, 800 psi

(C) Vertical strain distribution along horizontal axis at p=13,800 psi

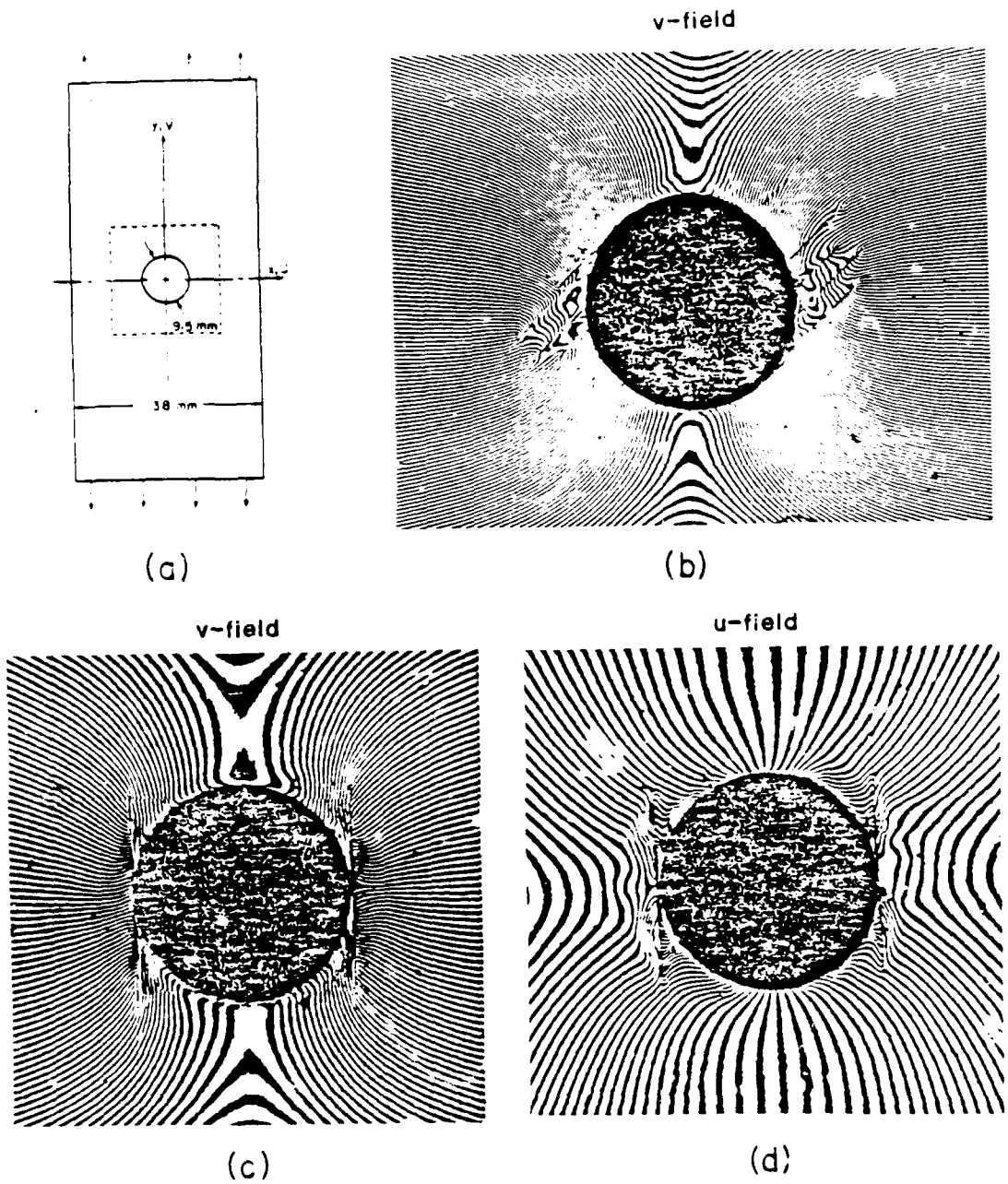

Figure 25. Displacement fields in fatigue - damaged graphite/epoxy composite specimen. (a) specimen geometry, (b) 45-deg. top ply, (c) and (d) O-deg. top ply (Ref. 49).

(a)

(b)

Figure 26. Residual deformation in a fatigued composite specimen, (a) V-displacement field, and (b) W-displacement field, (Ref. 50).

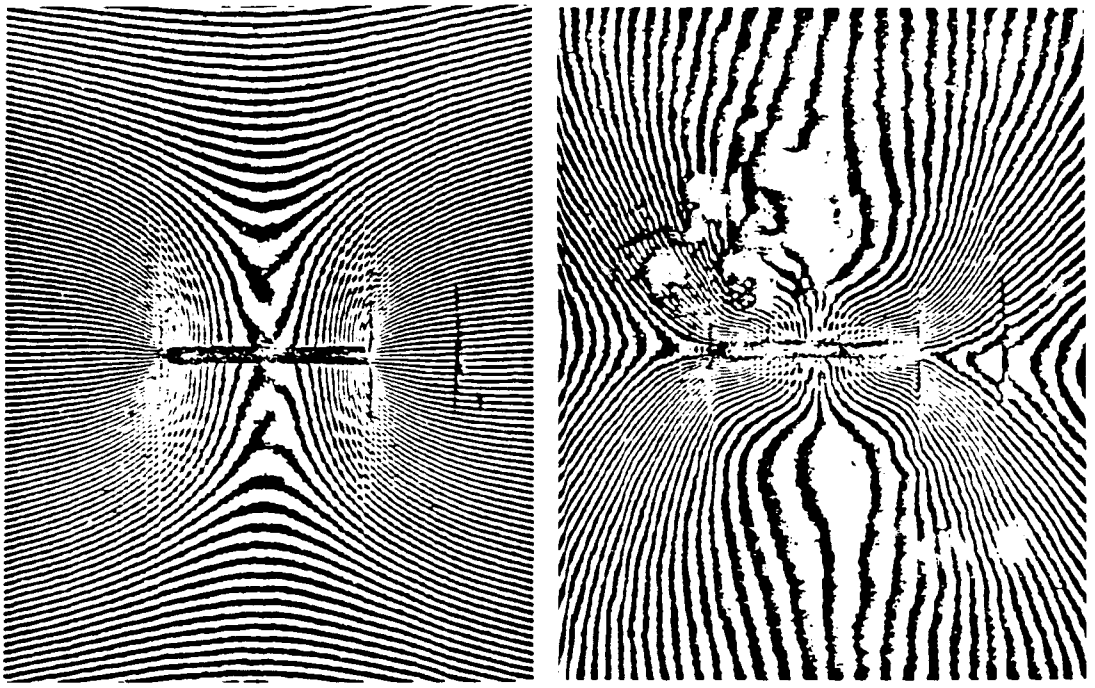

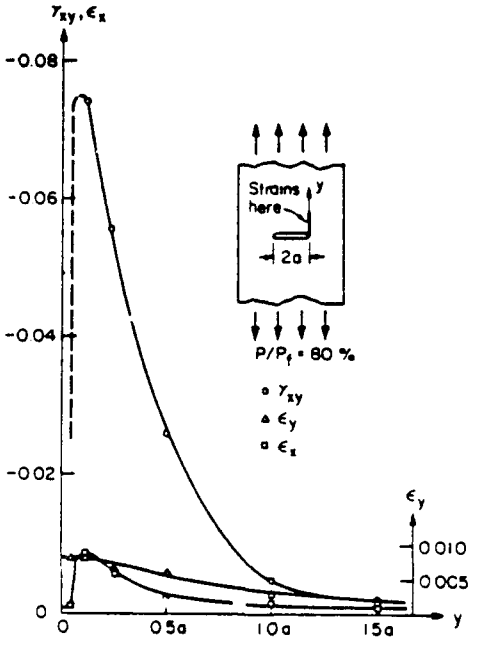

Figure 27. Displacement fringe patterns V (top left) and U (top right) for metal matrix specimen with a central slot, and normal and shear strains along the y-axis (bottom), (Ref. 51).

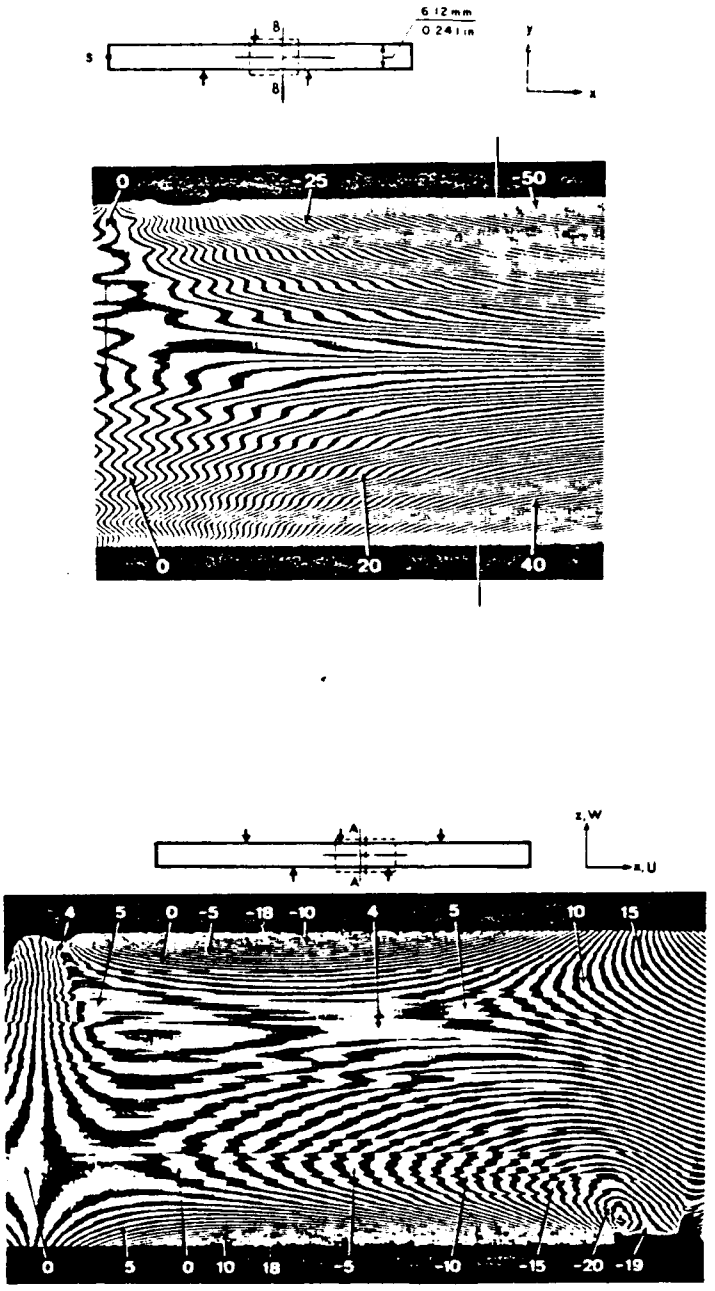

Figure 28. U-displacement field for quasi-isotropic composite in 3-point loading (top), and unidirectional composite in 5-point loading (bottom), (Ref. 57).

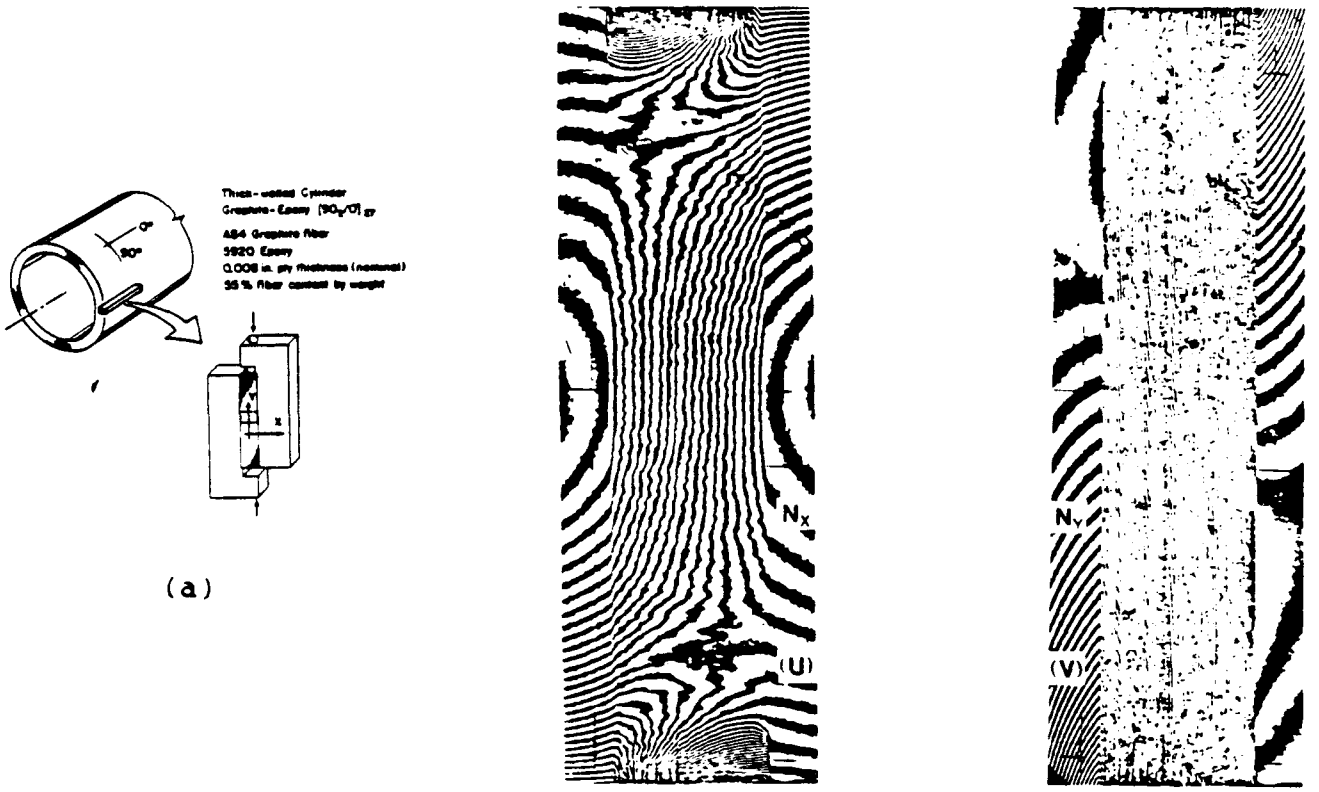

Figure 29. Rail shear loading, (a) specimen, (b) U and V fringe patterns, and (c) shear strains along individual plies, (Ref. 55).

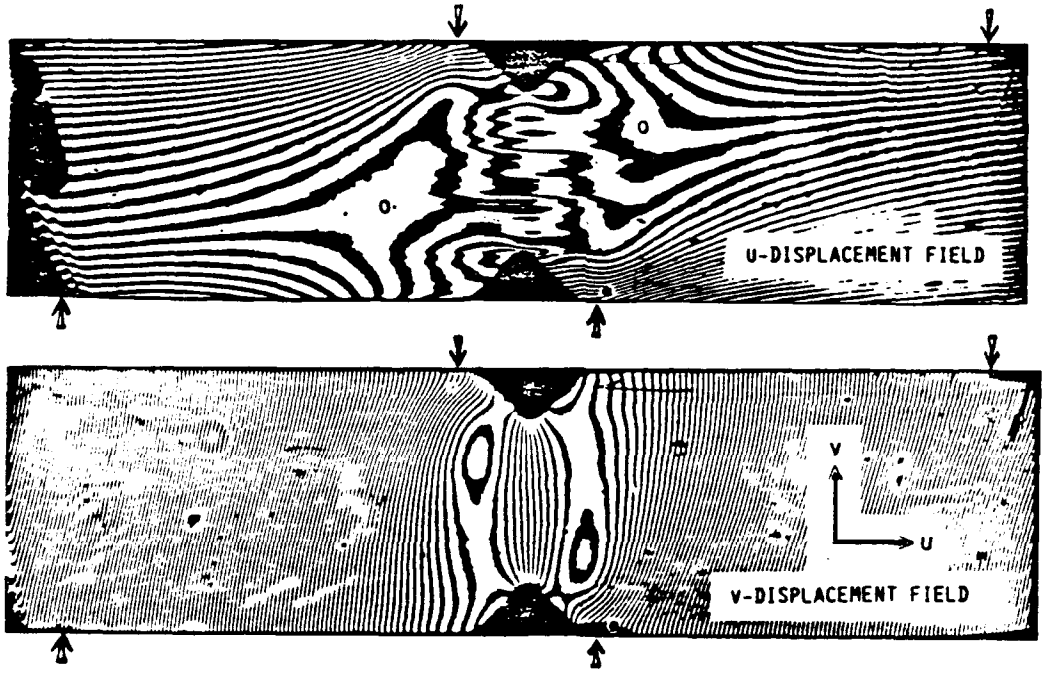

Moire' fringe pattern for the [0°] specimen

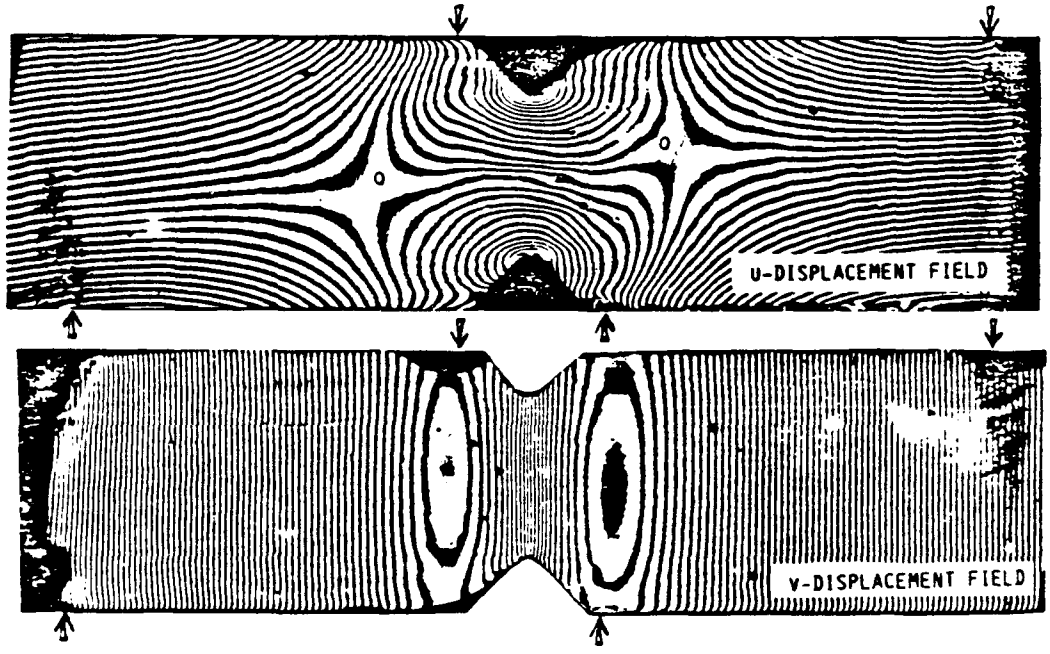

Moire' fringe pattern for the [0°/90°] specimen

Figure 30. Iosipescu shear specimen evaluation, (Ref. 56).

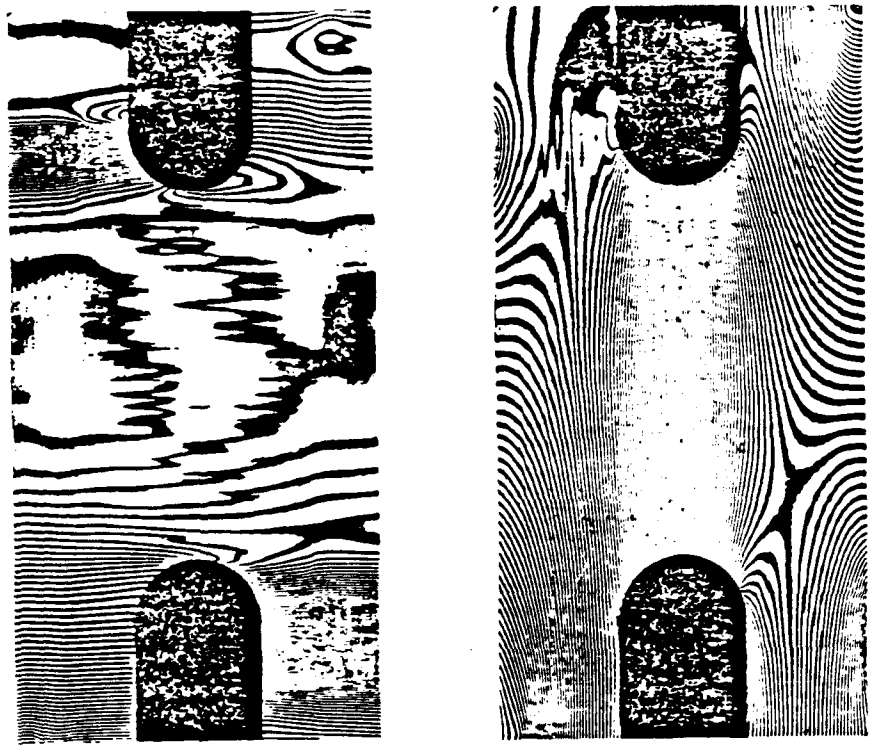

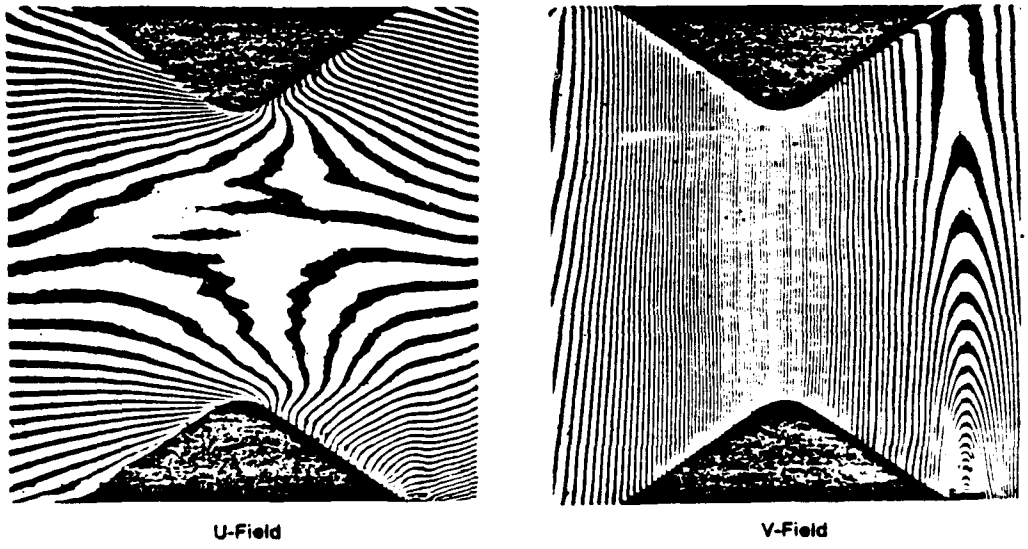

Figure 31. U and V displacement fringe patterns for double notched specimen (top), and Iosipescu specimen (bottom), (Ref. 57).

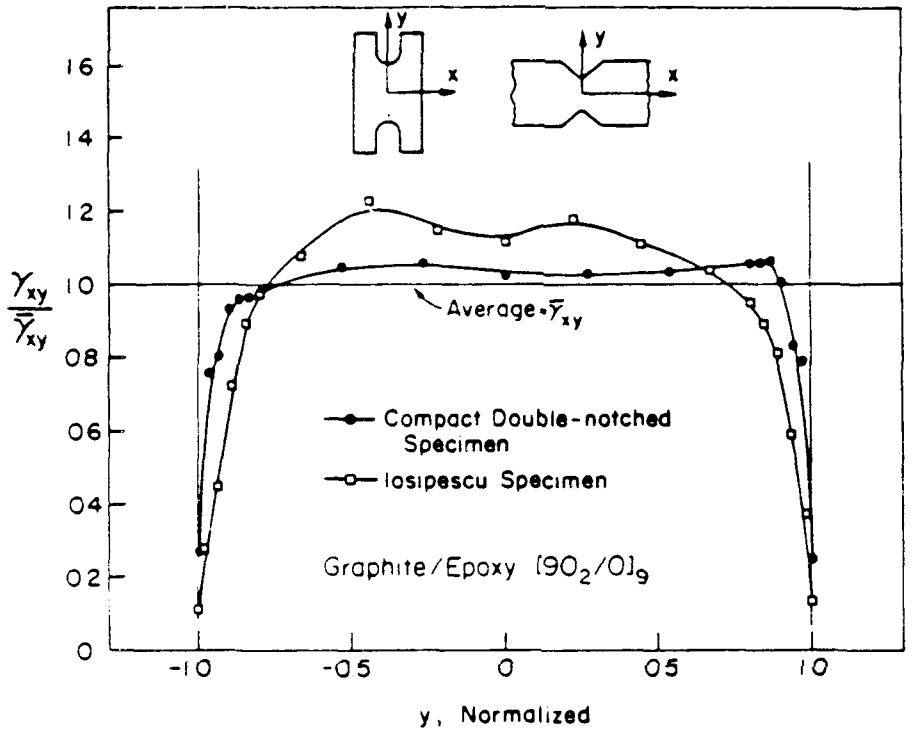

Figure 32. Shear strain distributions between notches for the compact double notched specimen and the Iosipescu specimen, (Ref. 57).

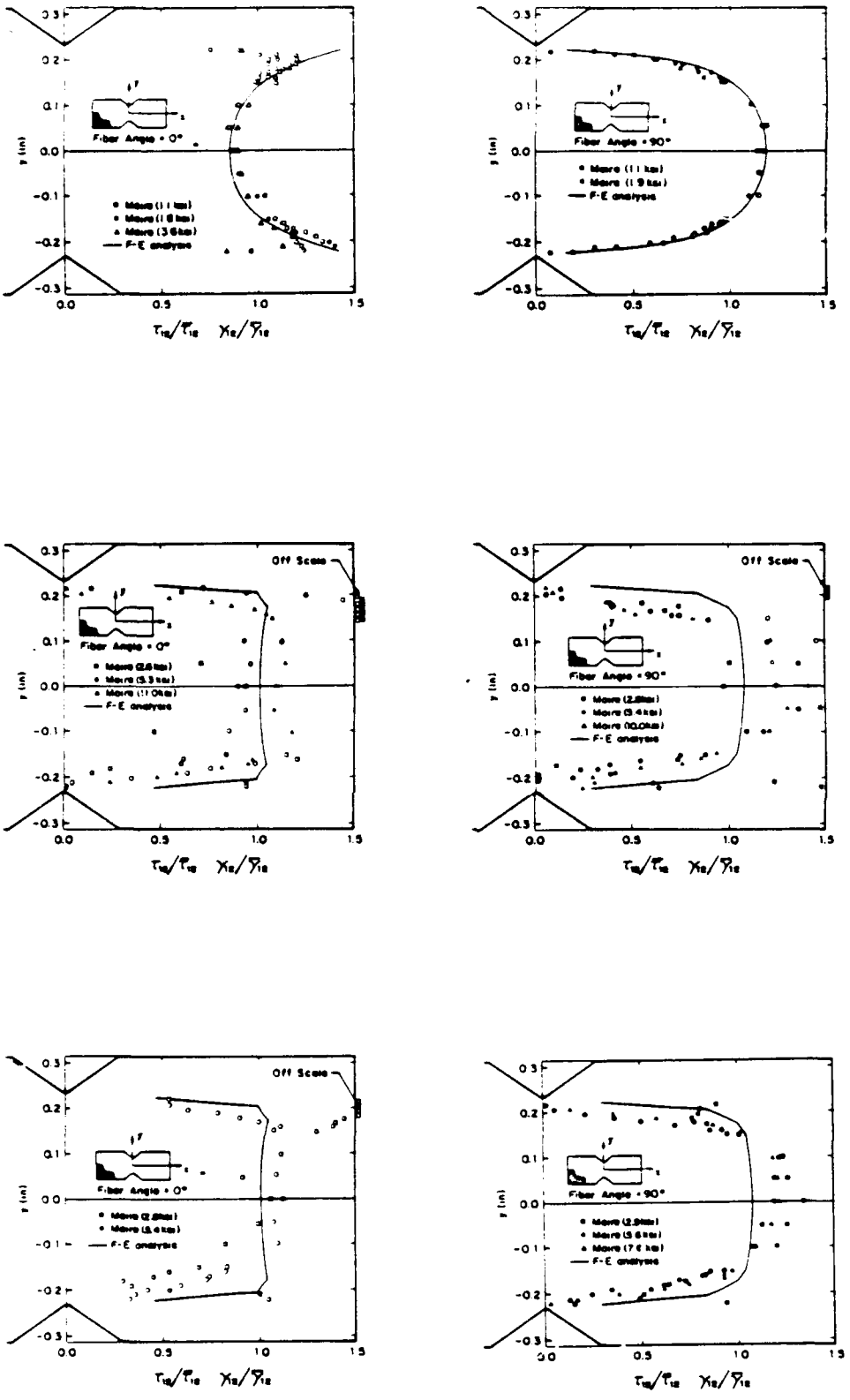

Figure 33. Shear stress and strain distributions for 0-deg. and 90-deg. Iosipescu specimen; graphite/epoxy (top), unannealed boron aluminum (center), and annealed boron aluminum (bottom), (Ref. 58).

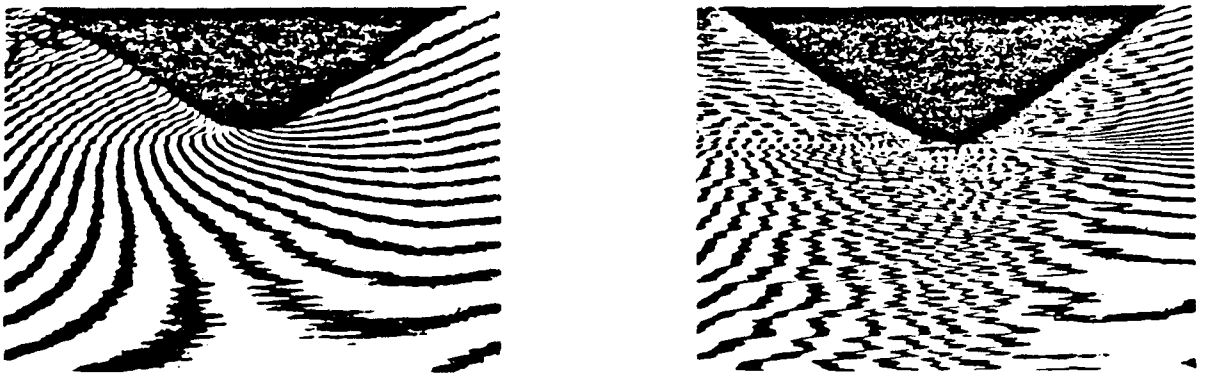

Figure 34. U-displacement field in the notch area of boron/aluminum 0-deg. Iosipescu specimens, (Ref. 58).

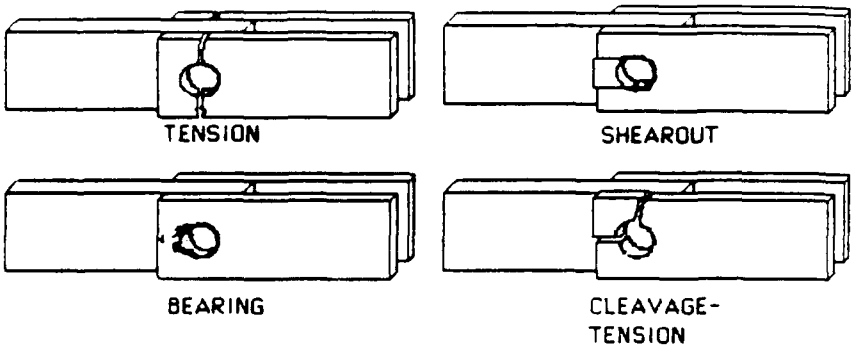

Figure 35. Failure modes in a single bolt joint, (Ref. 32).

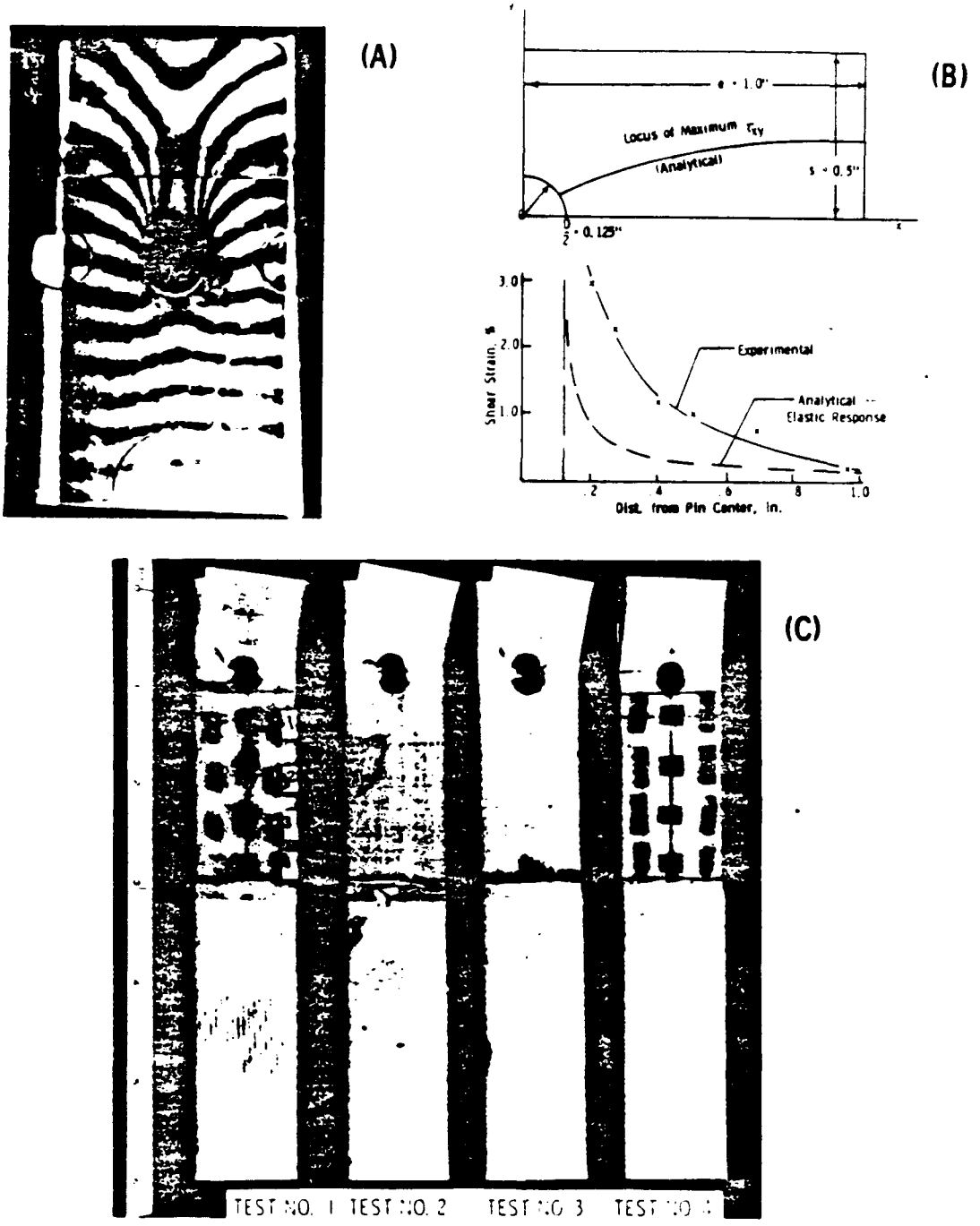

Figure 36. Results of moire experiments on pin-loaded 0/90-deg. glass/epoxy specimen, (Ref. 59); (A) - Moire axial displacement field, (B) - Comparison of predicted and measured shear strain distribution. (C) - Failure characteristics.

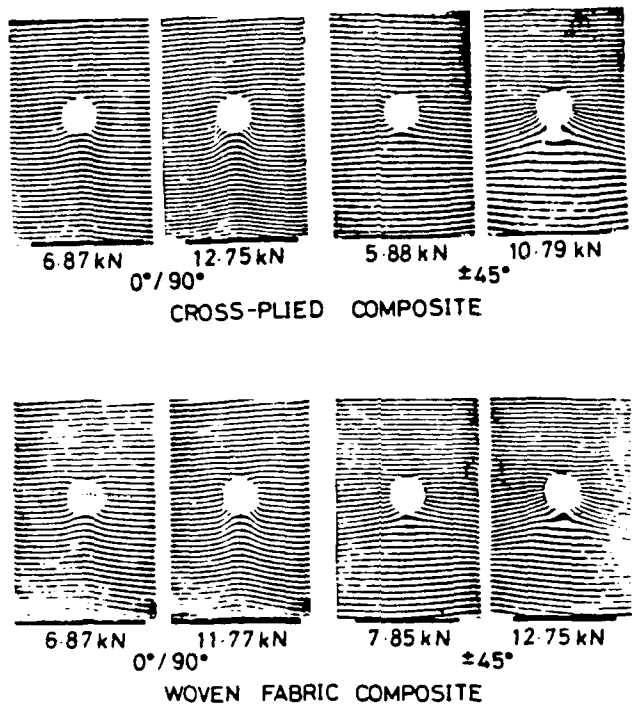

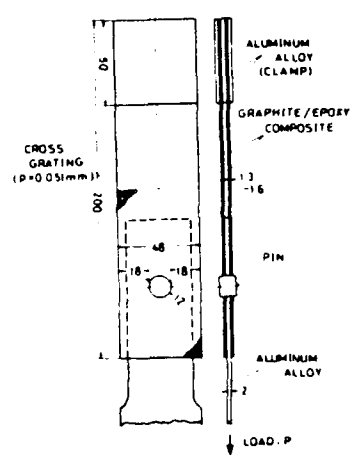

Figure 37. Cross-plied and woven fabric composites of 0/90-deg. and +45/-45-deg. laminates, moire fringe patterns, and specimen and loading geometry, (Ref. 60).

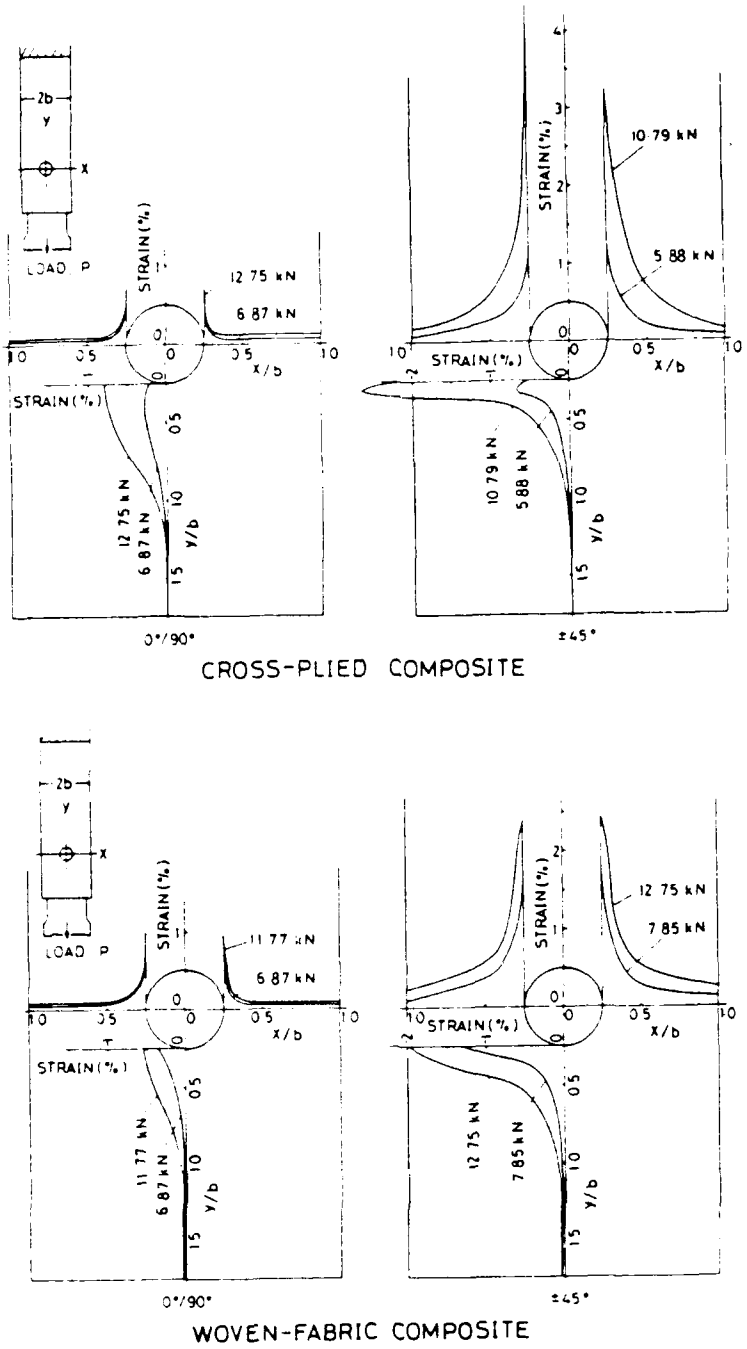

Figure 38. Strain distributions along x and y axes for cross-plied and woven fabric composites, (Ref. 60).

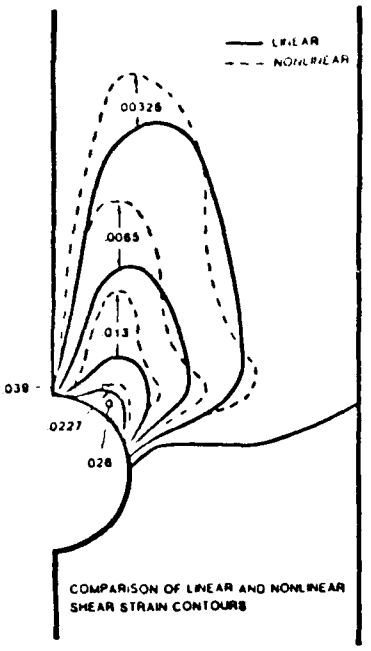

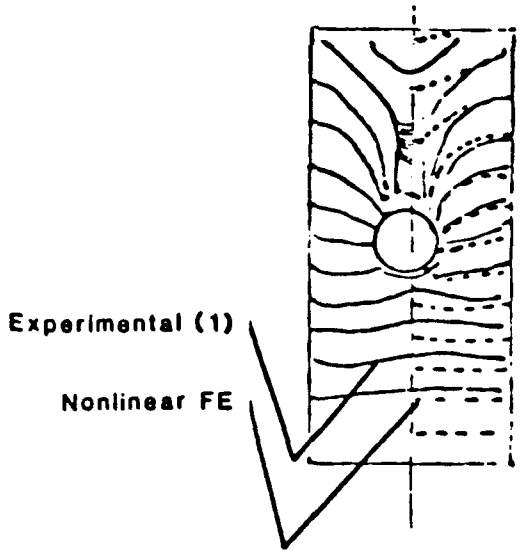

Figure 39. Experimental/numerical comparison of pin-loaded 0/90 glass/epoxy specimens, (Ref. 61).

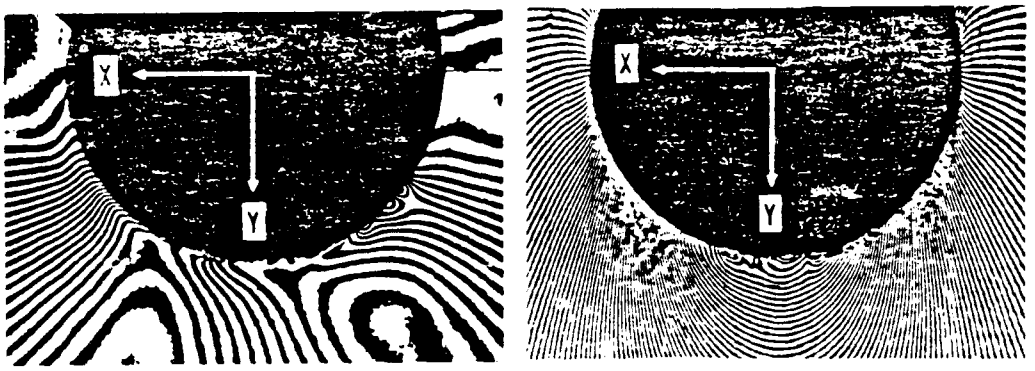

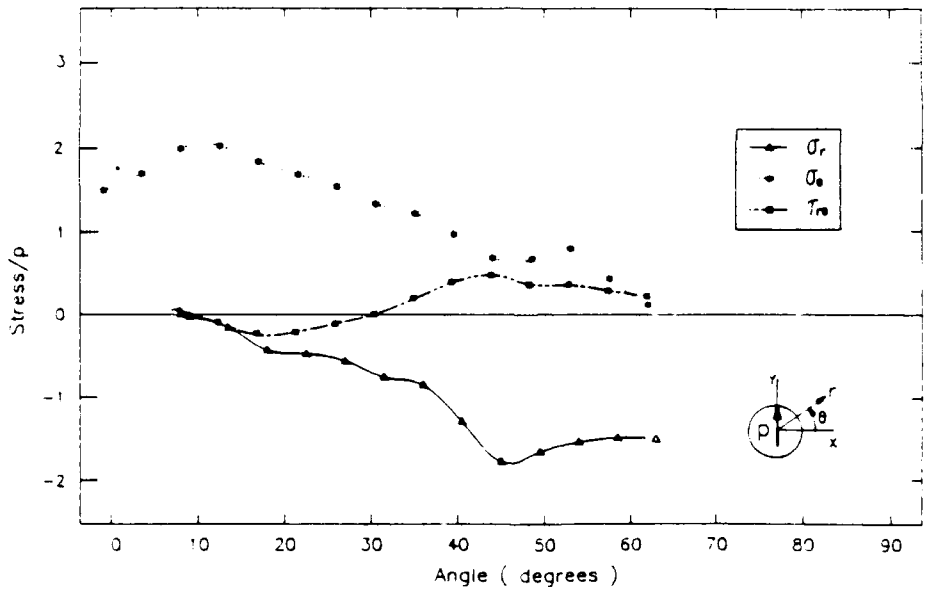

Figure 40. Moire fringe patterns of pin loaded graphite/epoxy specimen U-field (top left), V-field (top right), and contact stress distribution (bottom), (Ref. 62).

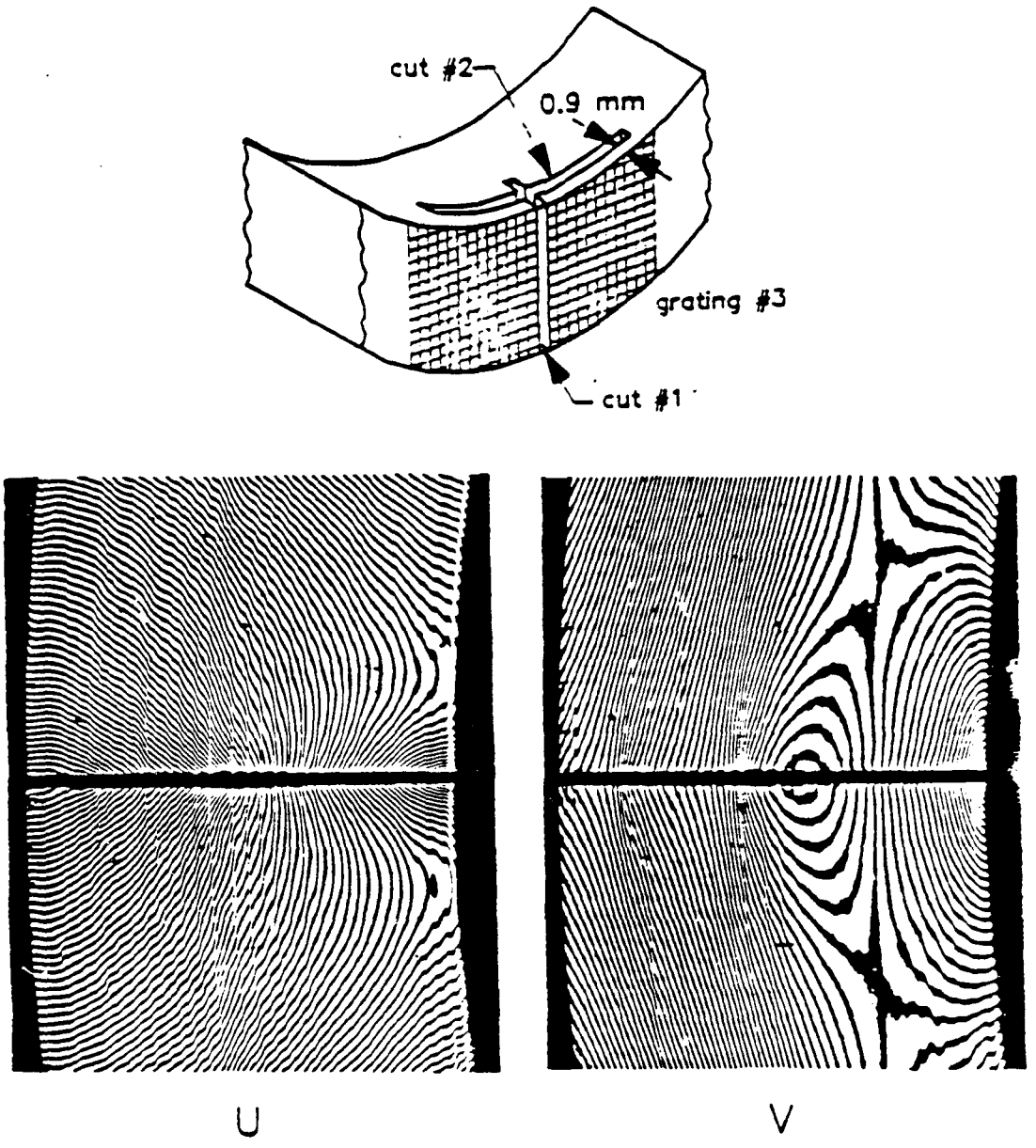

Figure 41. Residual strain, relieved by slicing and under-cutting a thick composite, (Ref. 69).

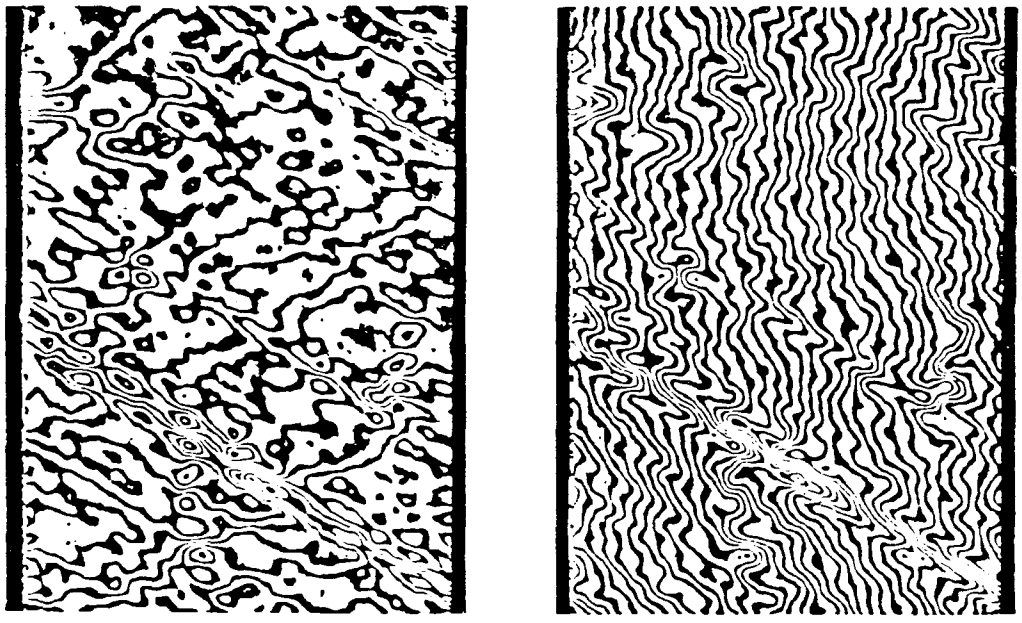

Figure 42. Moire fringe patterns representing nonuniformities of a tensile loaded panel, the fringe pattern on the right is a result of a small positive change of the reference grating, (Ref. 69).

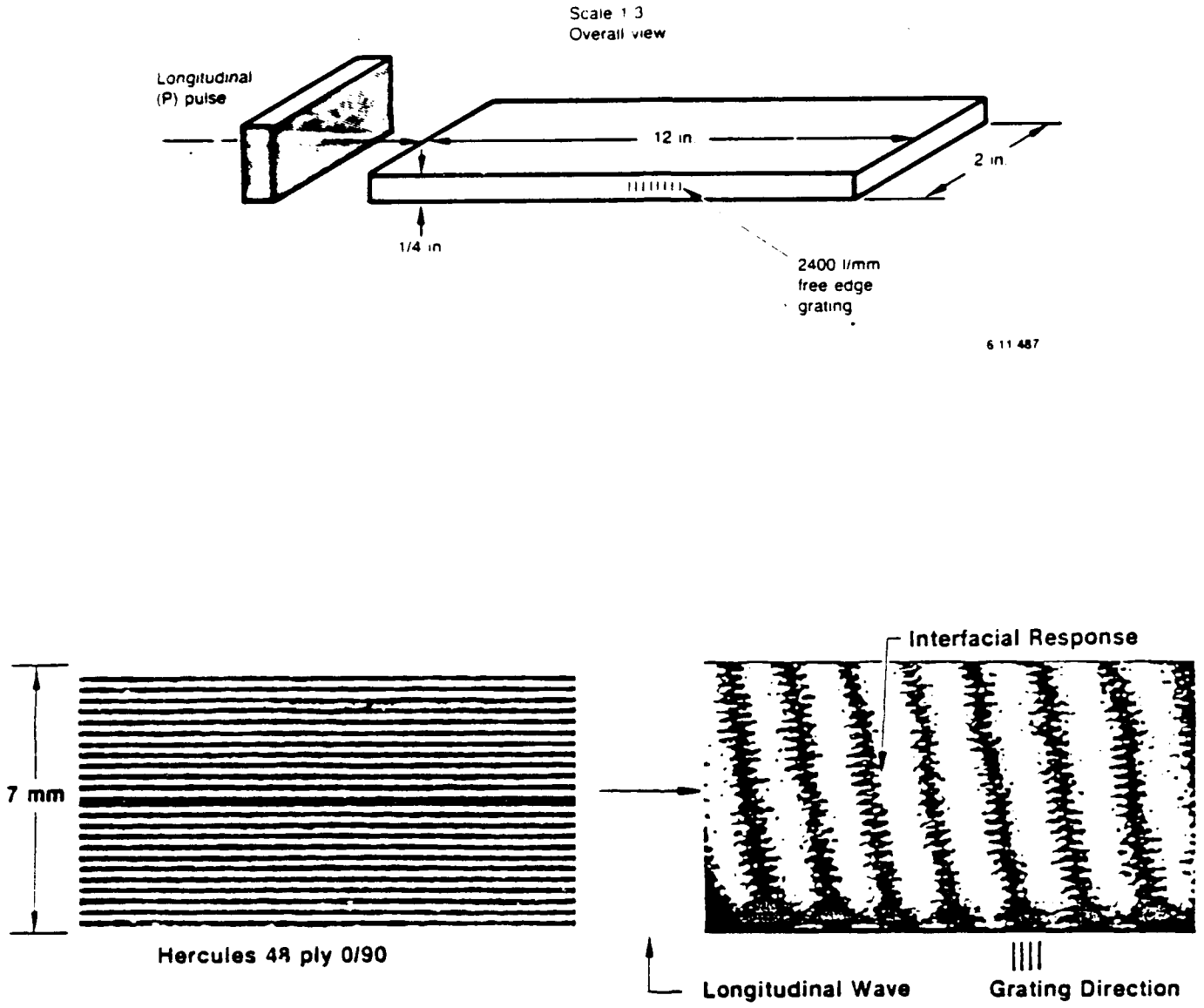

Figure 43. Transient wave propagation, impact geometry (top), and fringe patterns, before and after longitudinal pulse interaction, bottom left and bottom right respectively, (Ref. 71).

DISTRIBUTION LIST

No. of Copies	To
1	Office of the Under Secretary of Defense for Research and Engineering, The Pentagon, Washington, DC 20301
	Commander, U.S. Army Laboratory Command, 2800 Powder Mill Road, Adelphi, MD 20783-1145
1	ATTN: AMSLC-IM-TL
1	AMSLC-CT
	Commander, Defense Technical Information Center, Cameron Station, Building 5, 5010 Duke Street, Alexandria, VA 22304-6145
2	ATTN: DTIC-FDAC
1	MIA/CINDAS, Purdue University, 2595 Yeager Road, West Lafayette, IN 47905
	Commander, Army Research Office, P.O. Box 12211, Research Triangle Park, NC 27709-2211
1	ATTN: Information Processing Office
	Commander, U.S. Army Materiel Command, 5001 Eisenhower Avenue, Alexandria, VA 22333
1	ATTN: AMCSCI .
	Commander, U.S. Army Materiel Systems Analysis Activity, Aberdeen Proving Ground, MD 21005
1	ATTN: AMXSY-MP, H. Cohen
	Commander, U.S. Army Missile Command, Redstone Scientific Information Center, Redstone Arsenal, AL 35898-5241
1	ATTN: AMSMI-RD-CS-R/Doc
1	AMSMI-RLM
	Commander, U.S. Army Armament, Munitions and Chemical Command, Dover, NJ 07801
2	ATTN: Technical Library
	Commander, U.S. Army Natick Research, Development and Engineering Center, Natick, MA 01760-5010
1	ATTN: Technical Library
	Commander, U.S. Army Satellite Communications Agency, Fort Monmouth, NJ 07703
1	ATTN: Technical Document Center
	Commander, U.S. Army Tank-Automotive Command, Warren, MI 48397-5000
1	ATTN: AMSTA-ZSK
1	AMSTA-TSL, Technical Library
	Commander, White Sands Missile Range, NM 88002
1	ATTN: STEWS-WS-VT
	President, Airborne, Electronics and Special Warfare Board, Fort Bragg, NC 28307
1	ATTN: Library
	Director, U.S. Army Ballistic Research Laboratory, Aberdeen Proving Ground, MD 21005
1	ATTN: SLCBR-TSB-S (STINFO)
	Commander, Dugway Proving Ground, UT 84022
1	ATTN: Technical Library, Technical Information Division
	Commander, Harry Diamond Laboratories, 2800 Powder Mill Road, Adelphi, MD 20783
1	ATTN: Technical Information Office
	Director, Benet Weapons Laboratory, LCWSL, USA AMCCOM, Watervliet, NY 12189
1	ATTN: AMSMC-LCB-TL
1	AMSMC-LCB-R
1	AMSMC-LCB-RM
1	AMSMC-LCB-RP
	Commander, U.S. Army Foreign Science and Technology Center, 220 7th Street, N.E., Charlottesville, VA 22901-5396
3	ATTN: AIFRTC, Applied Technologies Branch, Gerald Schlesinger
	Commander, U.S. Army Aeromedical Research Unit, P.O. Box 577, Fort Rucker, AL 36360
1	ATTN: Technical Library

No. of Copies	To
	Commander, U.S. Army Aviation Systems Command, Aviation Research and Technology Activity, Aviation Applied Technology Directorate, Fort Eustis, VA 23604-5577
1	ATTN: SAVDL-E-MOS
	U.S. Army Aviation Training Library, Fort Rucker, AL 36360
1	ATTN: Building 5906-5907
	Commander, U.S. Army Agency for Aviation Safety, Fort Rucker, AL 36362
1	ATTN: Technical Library
	Commander, USACDC Air Defense Agency, Fort Bliss, TX 79916
1	ATTN: Technical Library
	Commander, Clarke Engineer School Library, 3202 Nebraska Ave., N. Ft. Leonard Wood, MO 65473-5000
1	ATTN: Library
	Commander, U.S. Army Engineer Waterways Experiment Station, P.O. Box 631, Vicksburg, MS 39180
1	ATTN: Research Center Library
	Commandant, U.S. Army Quartermaster School, Fort Lee, VA 23801
1	ATTN: Quartermaster School Library
	Naval Research Laboratory, Washington, DC 20375
1	ATTN: Code 5830
2	Dr. G. R. Yoder - Code 6384
	Chief of Naval Research, Arlington, VA 22217
1	ATTN: Code 471
1	Edward J. Morrissey, WRDC/MLTE, Wright-Patterson Air Force Base, OH 45433-6523
	Commander, U.S. Air Force Wright Research & Development Center, Wright-Patterson Air Force Base, OH 45433-6523
1	ATTN: WRDC/MLLP, M. Forney, Jr.
1	WRDC/MLBC, Mr. Stanley Schulman
	NASA - Marshall Space Flight Center, MSFC, AL 35812
1	ATTN: Mr. Paul Schuerer/EH01
	U.S. Department of Commerce, National Institute of Standards and Technology, Gaitherburg, MD 20899
1	ATTN: Stephen M. Hsu, Chief, Ceramics Division, Institute for Materials Science and Engineering
1	Committee on Marine Structures, Marine Board, National Research Council, 2101 Constitution Avenue, N.W., Washington, DC 20418
1	Materials Sciences Corporation, Suite 250, 500 Office Center Drive, Fort Washington, PA 19034-3213
1	Charles Stark Draper Laboratory, 68 Albany Street, Cambridge, MA 02139
	Wyman-Gordon Company, Worcester, MA 01601
1	ATTN: Technical Library
	General Dynamics, Convair Aerospace Division P.O. Box 748, Forth Worth, TX 76101
1	ATTN: Mfg. Engineering Technical Library
	Plastics Technical Evaluation Center, PLASTEC, ARDEC Bldg. 355N, Picatinny Arsenal, NJ 07806-5000
1	ATTN: Harry Pebly
1	Department of the Army, Aerostructures Directorate, MS-266, U.S. Army Aviation R&T Activity - AVSCOM, Langley Research Center, Hampton, VA 23665-5225
1	NASA - Langley Research Center, Hampton, VA 23665-5225
1	U.S. Army Propulsion Directorate, NASA Lewis Research Center, 2100 Brookpark Road, Cleveland, OH 44135-3191
1	NASA - Lewis Research Center, 2100 Brookpark Road, Cleveland, OH 44135-3191
	Director, U.S. Army Materials Technology Laboratory, Watertown, MA 02172-0001
2	ATTN: SLCMT-TML
1	Author

U.S. Army Materials Technology Laboratory
Watertown, Massachusetts 02172-0001
AN INTRODUCTION TO MOIRE METHODS WITH APPLICATIONS IN COMPOSITE MATERIALS -
Robert F. Anastasi

Technical Report MTL TR 92-55, August 1992, 55 pp- illus

AD_____
UNCLASSIFIED
UNLIMITED DISTRIBUTION

Key Words

Moire analysis
Composite materials
Optical methods

The moire effect or the fringe pattern formed by superimposing two arrays of dark and light line patterns is utilized in experimental mechanics to measure deformations of bodies subjected to external loads. Although mainly a laboratory tool the techniques have been applied to problems in the mechanics of composite materials to map strain concentrations around holes, cracks, and delamination, as well as examining edge effects, shearing deformation, and mechanically fastened composite material.

U.S. Army Materials Technology Laboratory
Watertown, Massachusetts 02172-0001
AN INTRODUCTION TO MOIRE METHODS WITH APPLICATIONS IN COMPOSITE MATERIALS -
Robert F. Anastasi

Technical Report MTL TR 92-55, August 1992, 55 pp- illus

AD_____
UNCLASSIFIED
UNLIMITED DISTRIBUTION

Key Words

Moire analysis
Composite materials
Optical methods

The moire effect or the fringe pattern formed by superimposing two arrays of dark and light line patterns is utilized in experimental mechanics to measure deformations of bodies subjected to external loads. Although mainly a laboratory tool the techniques have been applied to problems in the mechanics of composite materials to map strain concentrations around holes, cracks, and delamination, as well as examining edge effects, shearing deformation, and mechanically fastened composite material.

U.S. Army Materials Technology Laboratory
Watertown, Massachusetts 02172-0001
AN INTRODUCTION TO MOIRE METHODS WITH APPLICATIONS IN COMPOSITE MATERIALS -
Robert F. Anastasi

Technical Report MTL TR 92-55, August 1992, 55 pp- illus

AD_____
UNCLASSIFIED
UNLIMITED DISTRIBUTION

Key Words

Moire analysis
Composite materials
Optical methods

The moire effect or the fringe pattern formed by superimposing two arrays of dark and light line patterns is utilized in experimental mechanics to measure deformations of bodies subjected to external loads. Although mainly a laboratory tool the techniques have been applied to problems in the mechanics of composite materials to map strain concentrations around holes, cracks, and delamination, as well as examining edge effects, shearing deformation, and mechanically fastened composite material.

U.S. Army Materials Technology Laboratory
Watertown, Massachusetts 02172-0001
AN INTRODUCTION TO MOIRE METHODS WITH APPLICATIONS IN COMPOSITE MATERIALS -
Robert F. Anastasi

Technical Report MTL TR 92-55, August 1992, 55 pp- illus

AD_____
UNCLASSIFIED
UNLIMITED DISTRIBUTION

Key Words

Moire analysis
Composite materials
Optical methods

The moire effect or the fringe pattern formed by superimposing two arrays of dark and light line patterns is utilized in experimental mechanics to measure deformations of bodies subjected to external loads. Although mainly a laboratory tool the techniques have been applied to problems in the mechanics of composite materials to map strain concentrations around holes, cracks, and delamination, as well as examining edge effects, shearing deformation, and mechanically fastened composite material.